The Symbiotic Stars

Augustin Skopal

Astronomical Institute, Slovak Academy of Sciences, Tatranská Lomnica, Slovakia

1. Introduction to symbiotic stars
   - orbital & physical parameters; observational characteristics
2. Multiwavelength modeling the composite continuum
   - composite spectrum, physical parameters, ion. structure.
3. Mass-transfer problem in symbiotic stars
4. Thermonuclear outbursts & jets
   - from accretion-powered SySts to nova outbursts
   - from (symbiotic) nova outbursts to Z And-type outbursts
5. Challenges for future work

Supported by the APVV contract No. APVV-20-0148

and by the SAS VEGA grant No. 2/0030/21

APVV

SKALNATÉ PLESO

Introduction – a brief history

Fleming, W. (1912) - a list of “stars with peculiar spectra” (stellar continuum and emission lines; Z And, SY Mus)
Further studies by Cannon, Merrill (1919), Plaskett (1928), Hogg (1932).

Merrill & Humason (1932) - three new "stars with combination spectra", CI Cyg, RW Hya and AX Per – now well-known SySts.

Merrill (1958) for the first time used the name "symbiotic stars" for this group of stars (features of red giants and planetary nebulae).

1978 – The launch of the IUE satellite: the presence of a very hot star in the UV spectrum (1200 - 3500 A) – *the binary nature of SySts.*

Friedjung and Viotti, 1982 - The first conference: "The nature of SySts"

Allen (1984) - The first catalog and spectral atlas of known SySts.

Seaquist et al. (1984) - Modeling the ionization structure of SySts.

Kenyon, 1986 - The first monograph summarizing the current view at that time.

Introduction - basic characteristics

Wide interacting binary systems: Red giant + White dwarf (or NS)

P_{orb} ~ 100 x (days – years); typical values are 1 – 3 years

Basic interaction: Mass loss from the RG + Accretion by the WD

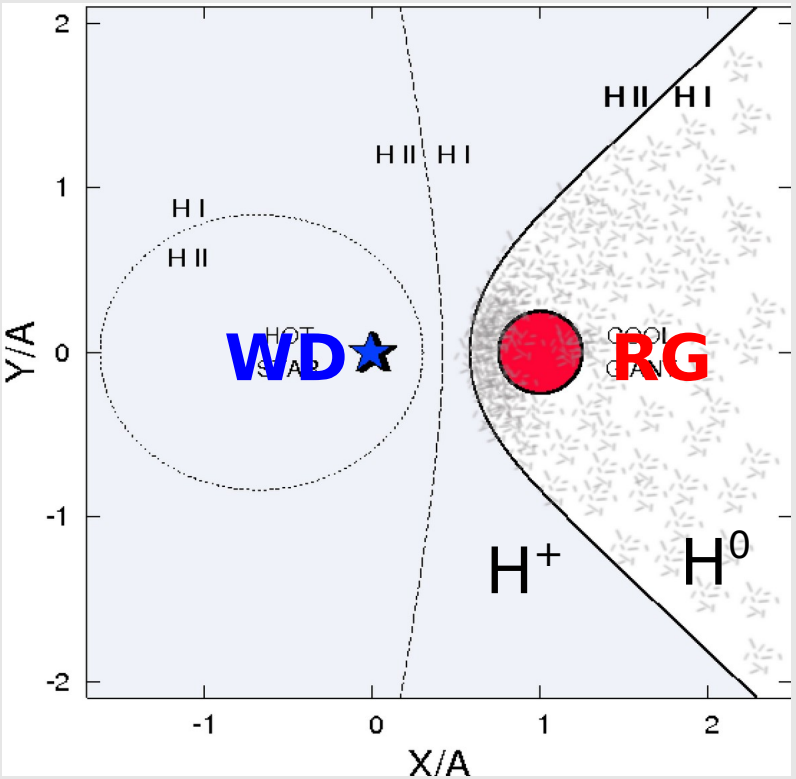

Accretion from the RG wind
(at 10^{-8}–10^{-7} M_{Sun}/yr)
==>
Hot & Luminous WD
==>
Ionization of the RG wind
==>
Symbiotic nebula

Figure: Ionization structure of SySts during quiescent phase. Stationary case for H: The wind from the RG is ionized by the hot WD radiation. According to Seaquist et al. 1984, ApJ, 284, 202.

Observational characteristics – spectroscopy

Emission lines of low & highly ionized elements:
(i) Low ionization: H I, He I, Fe II, Ti II,..., [OI], [NII]
(ii) High ionization: He II, NIII, [OIII], [FeVII], OVI

BF Cyg: P=757 d; M5III + WD: HI, HeI, FeII, NIII, CIII, (HeII) & [OI], [FeII], [OIII]

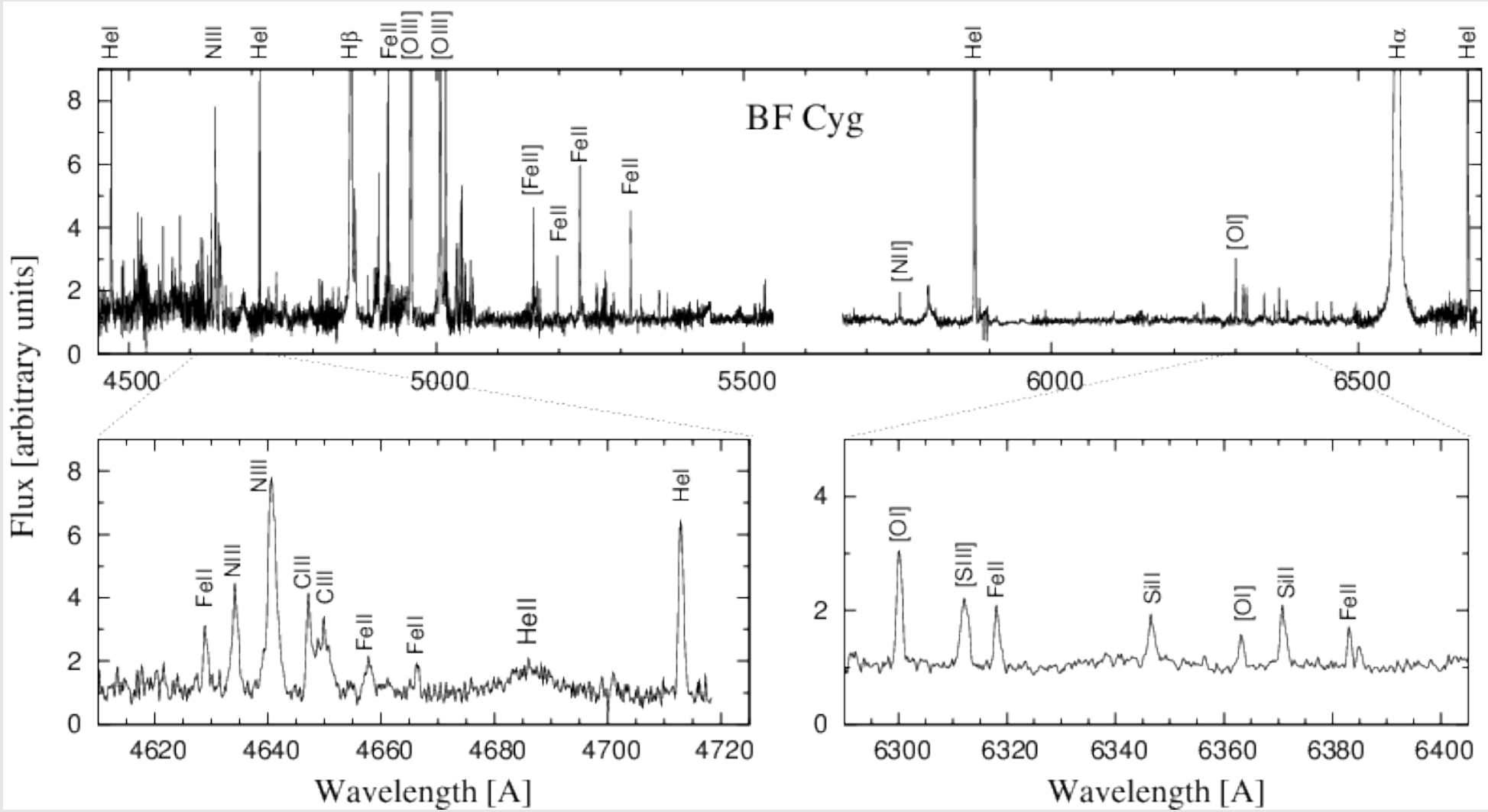

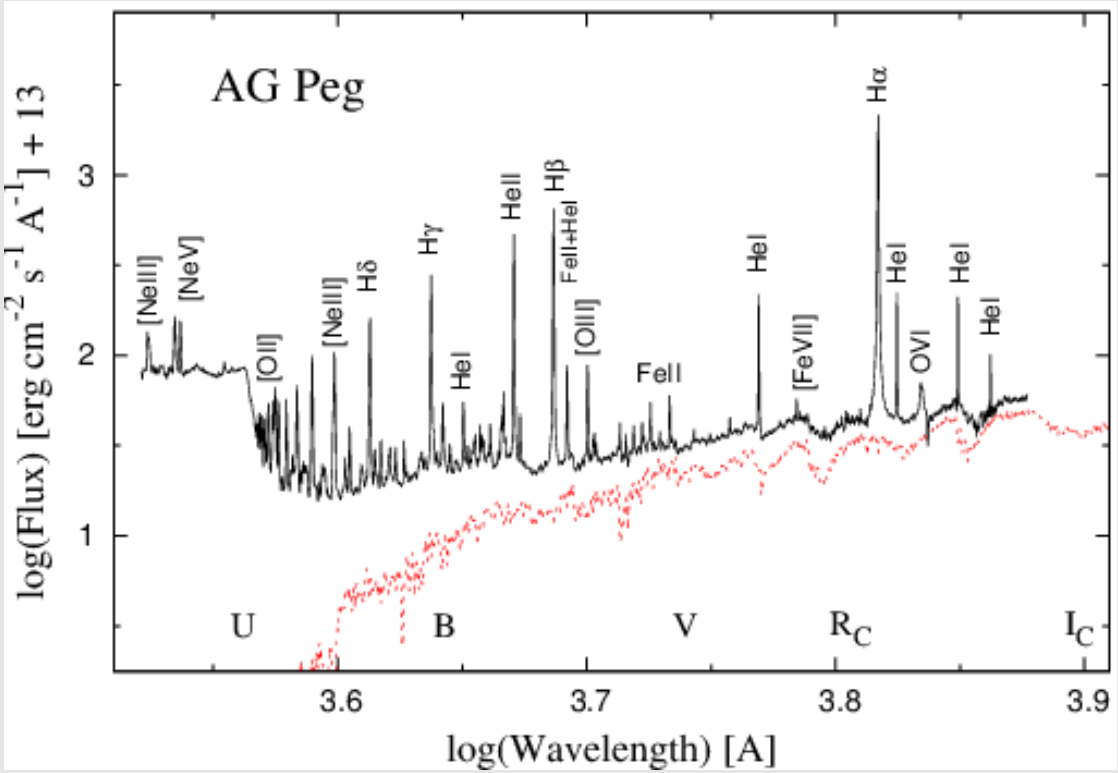

AG Peg: P=820 d; M2III + WD

Emission lines of low & high ionization elements:

FeII, HeI & HeII, OVI

[OI], [OIII] & [NeV], [FeVII]

+ nebular continuum

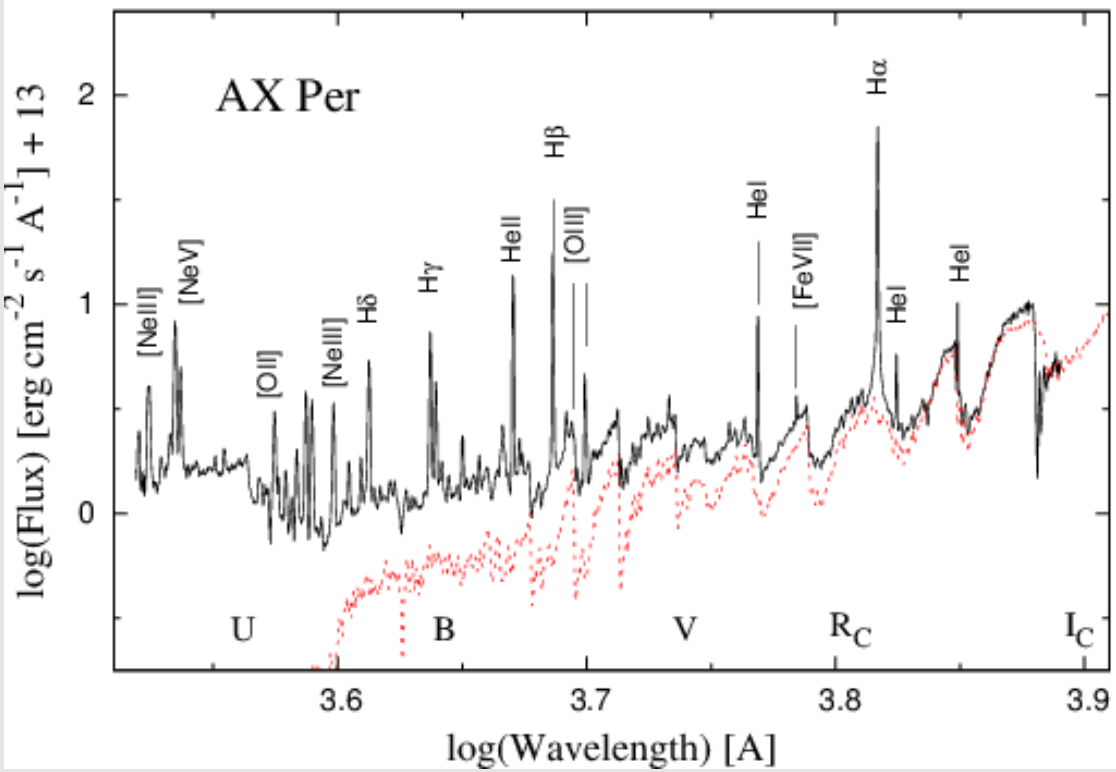

AX Per: P=680 d; M4.5III + WD

Emission lines of low & high ionization elements:

FeII, HeI & HeII, no OVI

[OI], [OII], [OIII] & [NeV], [FeVII]

+ nebular & warm stellar cont.

Observational characteristics – photometry

1. Z And-type outbursts & Quiescent phases

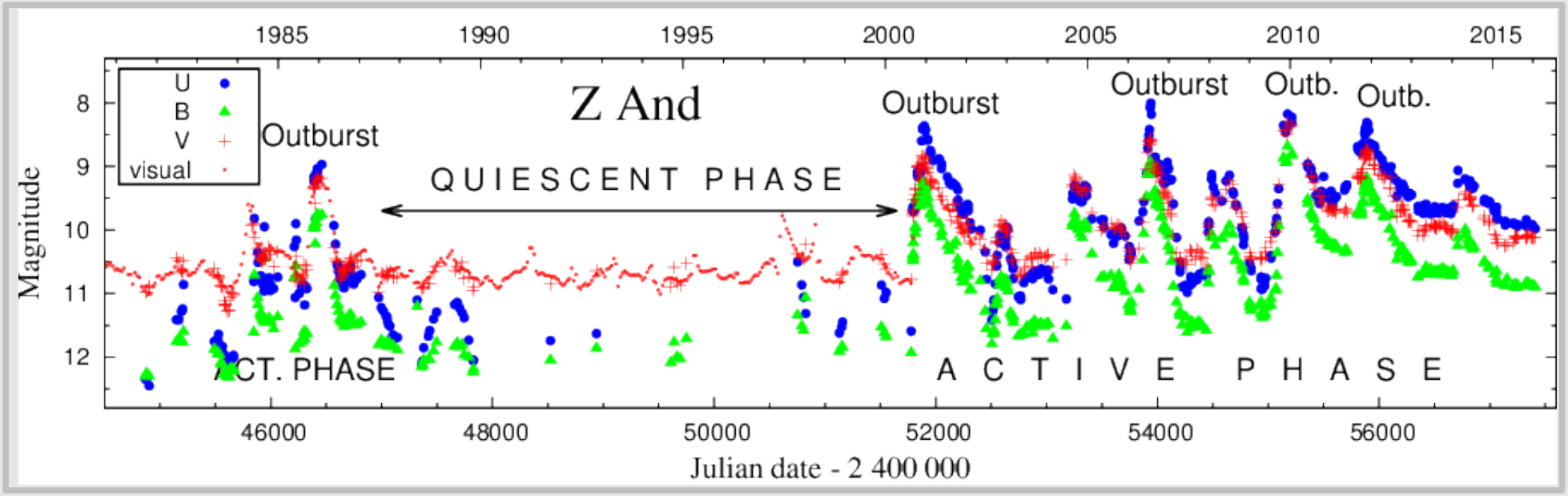

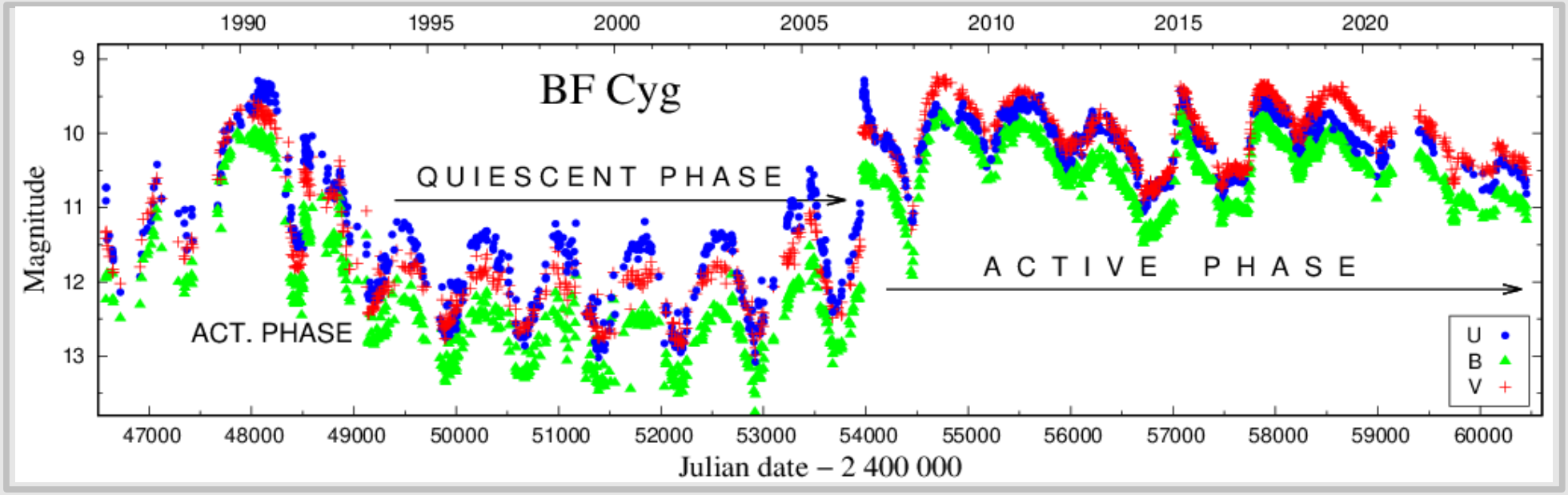

Wave-like orbital-related variation signals $L_{WD} \sim$ **a few** $\times 10^{36}$ erg/s, $(EM \sim 10^{59} - 10^{60}\,\mathrm{cm}^{-3})$, which requires $\dot{M}_{acc} \sim \dot{M}_{stable}$.

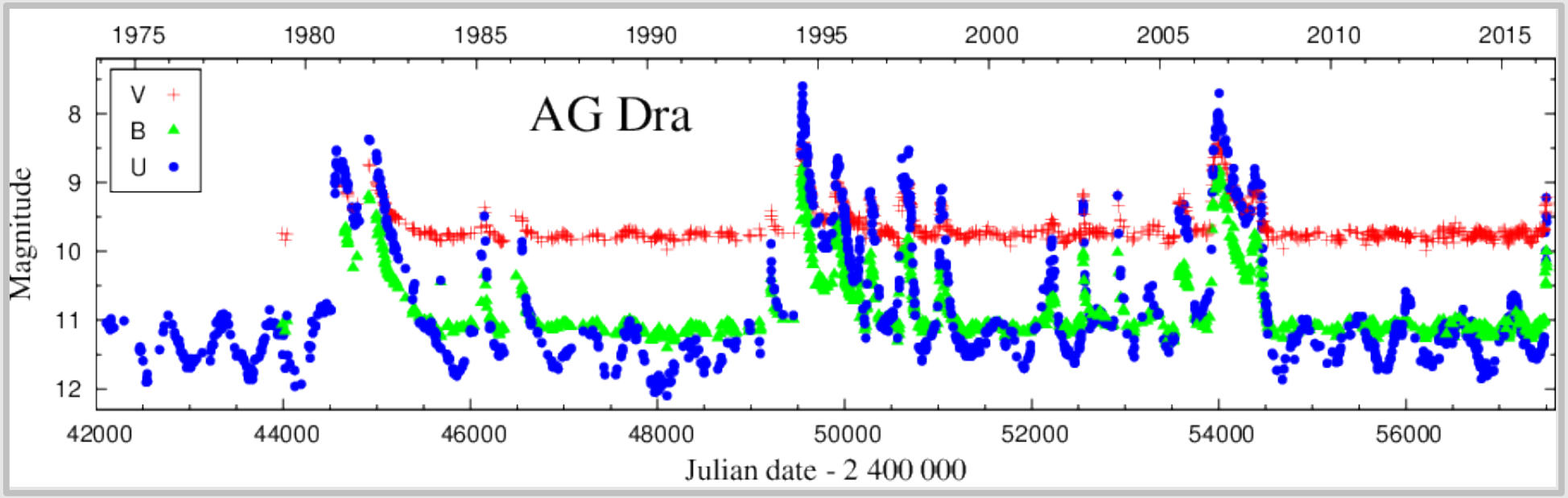

Basic types of variability in the optical continuum:

Quiescent phases: 1. Wave-like orbitally-related variation: apparent changes of the nebular emission, which is partially optically thick.

Active phases: 2. 1– 3 mag brightening. Z And-type outbursts.

Transition phases: 3. Apparent changes in P_{orb}: caused by dilution/creation of the warm photosphere that shifts the light minimum from the spectroscopic conjunction.

Observational characteristics – scattering processes

SySts represent ideal medium for **Rayleigh and Raman** scattering processes, because of simultaneous presence of neutral atoms and high energy photons.

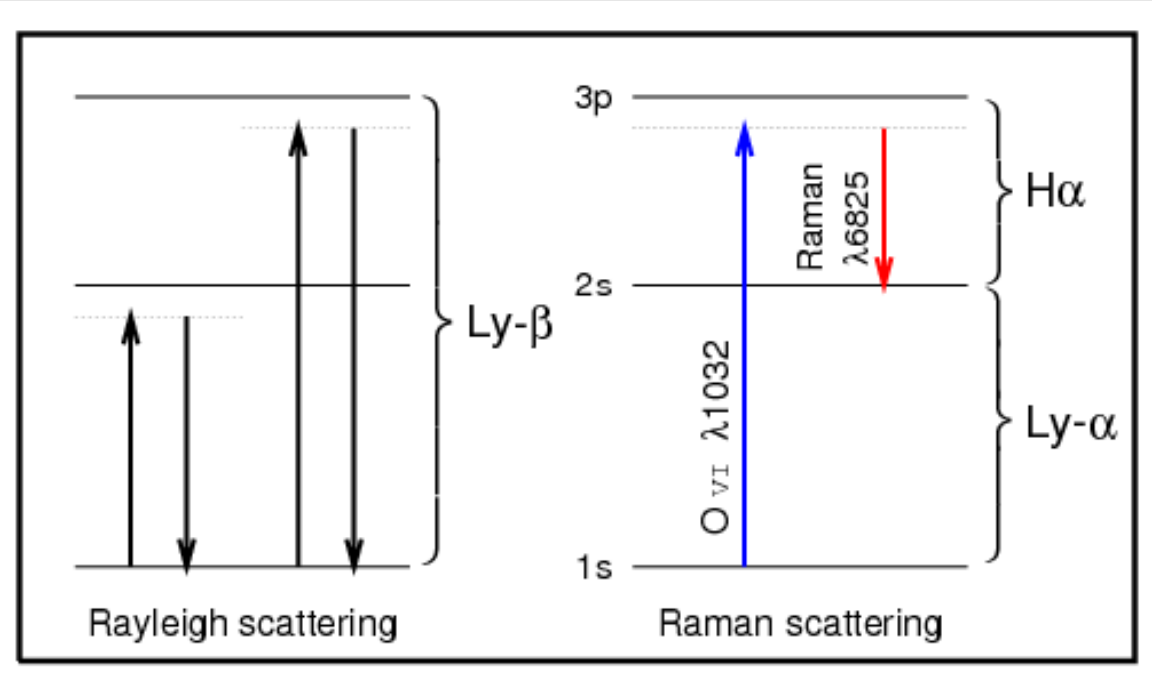

cross-sections σ:

$$\sigma_{Ray}(1032) = 34 \times \sigma_e$$
$$\sigma_{Ram}(1032) = 6.6 \times \sigma_e$$
$$\sigma_e = 6.65 \times 10^{-25} cm^2$$

Schmidt (1989, A&A, 211, L31)
Nussbaumer et al. (1989, A&A, 211, L27)

Left: Schematic energy level diagram for Rayleigh scattering around Ly-α and Ly-β.
Right: Raman scattering of OVI 1032A photons by neutral hydrogen.

Intermedial levels around main levels are very unstable. Electron captured at the intermedial level is immediately stabilized by a transition to a main level.

Rayleigh scattering can strongly attenuate the continuum around hydrogen Lyman lines.

Example of quiescent phase

The Rayleigh scattering can be observed only if the line-of-sight intersects the neutral region, which is around inferior conjunction of the giant during quiescence.

Quiescent SySt EG And:
The continuum around Ly-α is Rayleigh attenuated with N_H = 9.4E+22 cm^{-2} .

Raman scattering converts the far-UV photons around, e.g., Ly-β to the optical. Example of OVI 1032 --> 6825 Raman conversion.

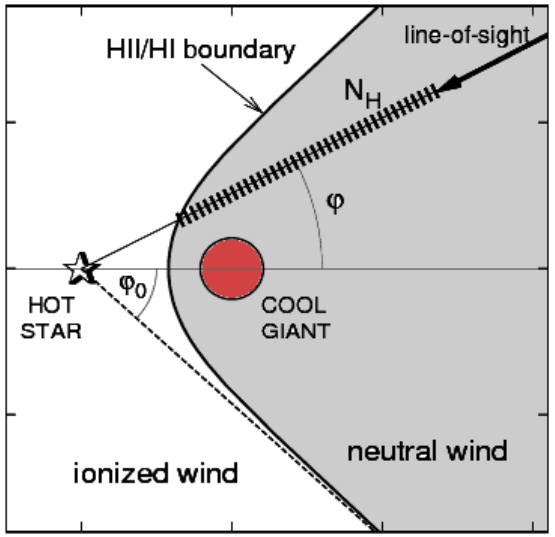

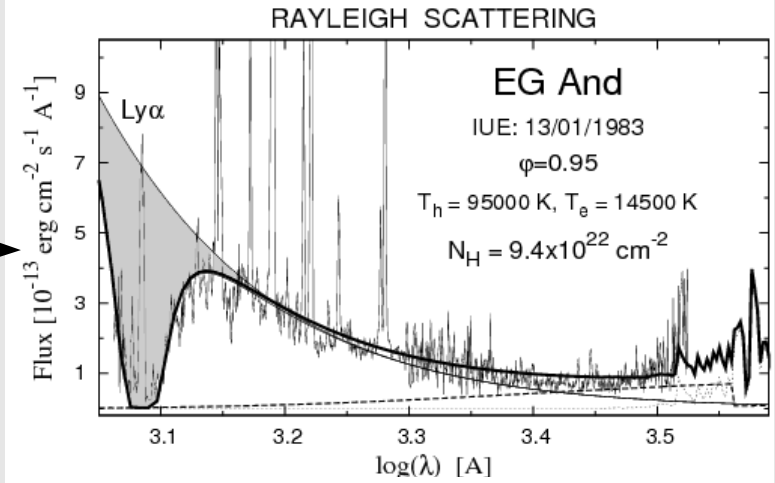

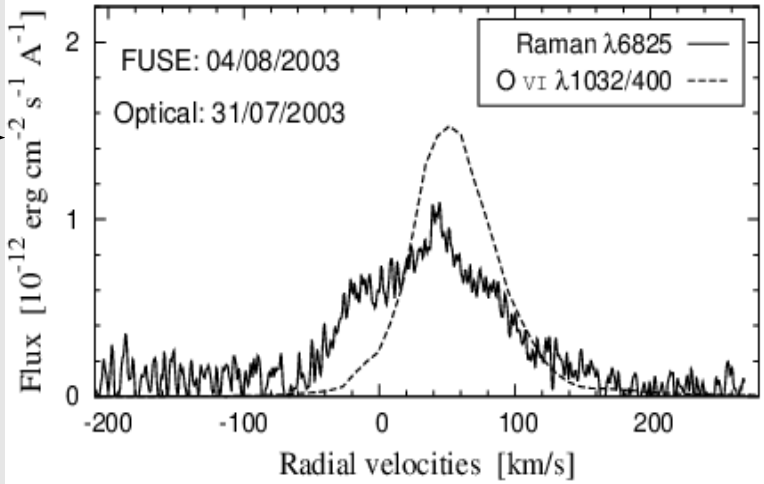

Multiwavelength modeling the composite continuum of SySts

Different components of radiation evolving in time

Multiwavelength modeling the composite continuum

$$F(\lambda) = F_{WD}(\lambda) + F_N(\lambda) + F_G(\lambda) + F_D(\lambda)$$

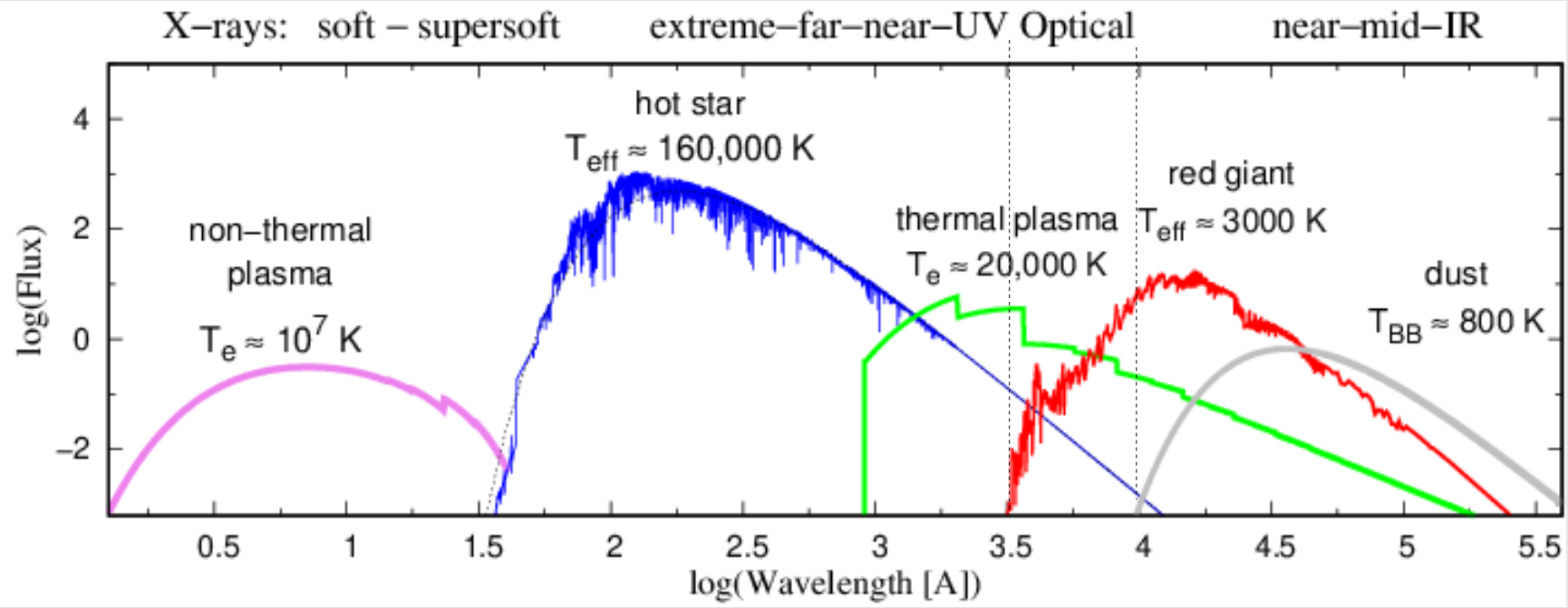

Aim: disentangling the composite spectrum to obtain physical parameters of individual components of radiation

X-ray – IR SED
Example of the symbiotic star RR Tel

d=2.6 kpc

Symbiotic nova, 1944, still burning

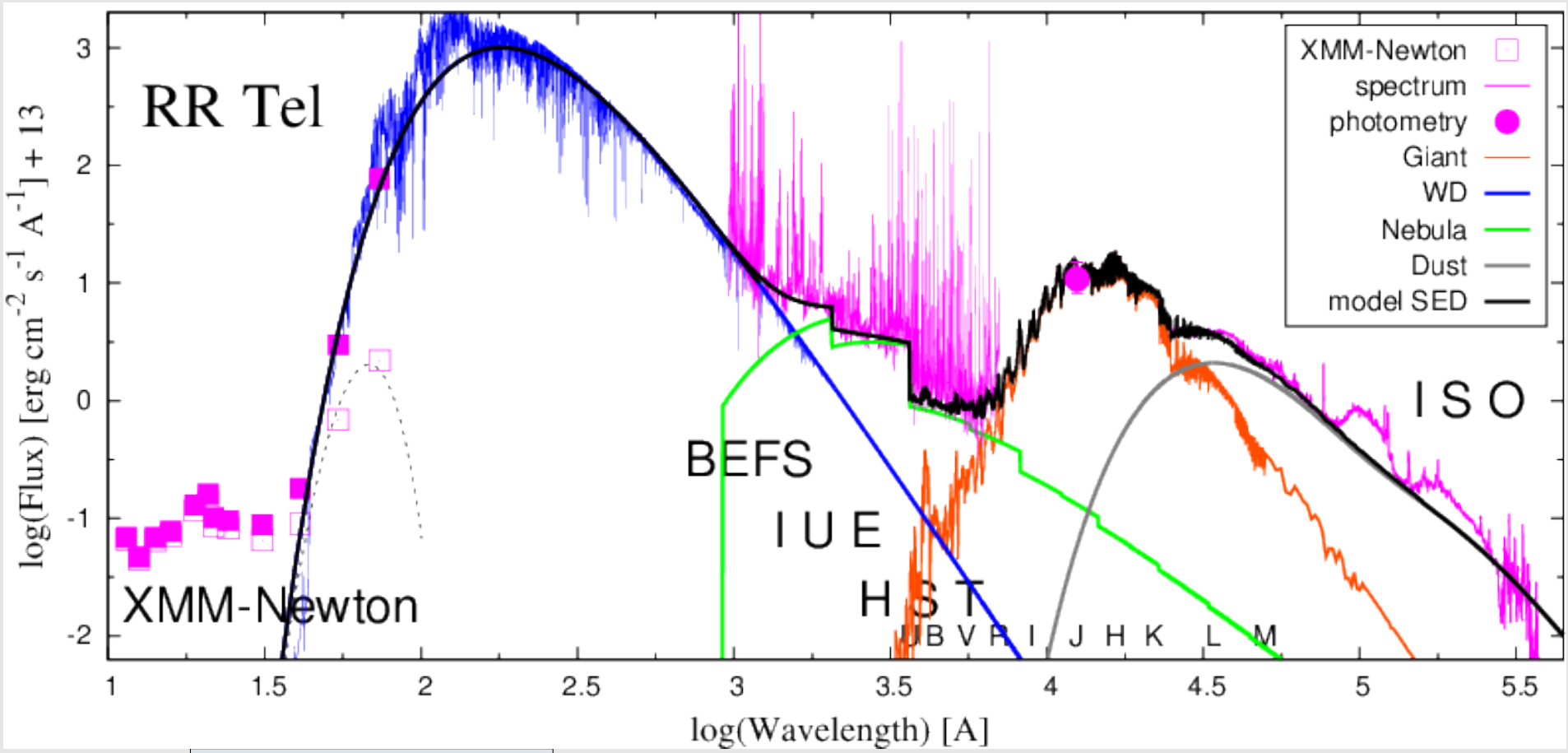

Hot plasma:
$T \sim 0.6$
$+ 1.7\ MK$

White dwarf:
$L_h = 5900\, L_{Sun}$
$T_h = 160000\ K$
$R_h^{eff} = 0.1\, R_{Sun}$
$N_H = 2.6 \times 10^{20}\ cm^{-2}$

Nebula:
$EM = 8.0 \times 10^{59}\ cm^{-3}$
$T_e = 26000\ K,$
$a(He\ II) \sim 0.08$

Giant:
$L_G = 3700\, L_{Sun}$
$T_{eff} = 2700\ K$
$R_G = 280\, R_{Sun}$

Dust:
$L_D = 2100\, L_{Sun}$
$T_D = 850\ K$
$R_D^{eff} = 2100\, R_{Sun}$

XMM-Newton: Gonzalez-Riestra et al. 2013, A&A, 556, A85; model SED: Credit A. Skopal

Near-IR SED: Two types of symbiotic stars:

1. S-type (stellar; ~80 %)

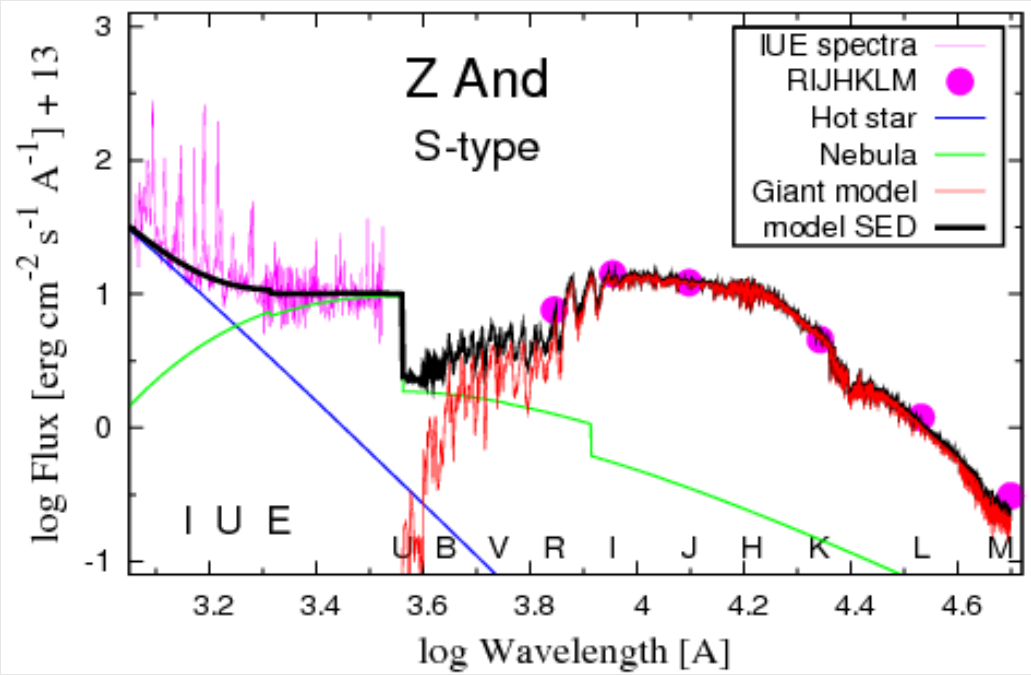

2. D-type (dusty; ~20%)

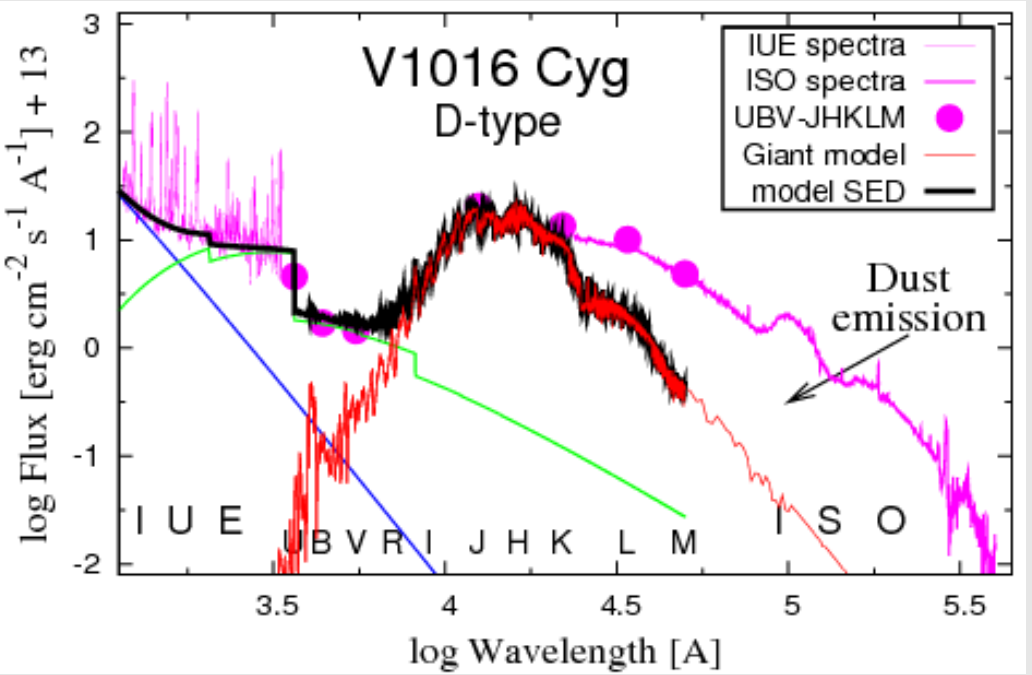

S-types:
Cool component – a normal M-type giant
Stellar type of the IR continuum.
No strong dust emission.
(if G-K giant – Yellow symbiotic stars)

D-types:
Cool component – a Mira-variable
Strong near-IR dust emission.
Called as *Symbiotic Miras*
P_{orb} - a few x (10–100) yr; unknown

(Webster & Allen, 1975, MNRAS, 171, 171; Kenyon et al., 1988, AJ, 95, 1817; Seal, 1990, Ap&SS, 174, 321)

Symbiotic stars as supersoft X-ray sources

X-ray / near-IR SED of AG Dra

d = 1.1.kpc

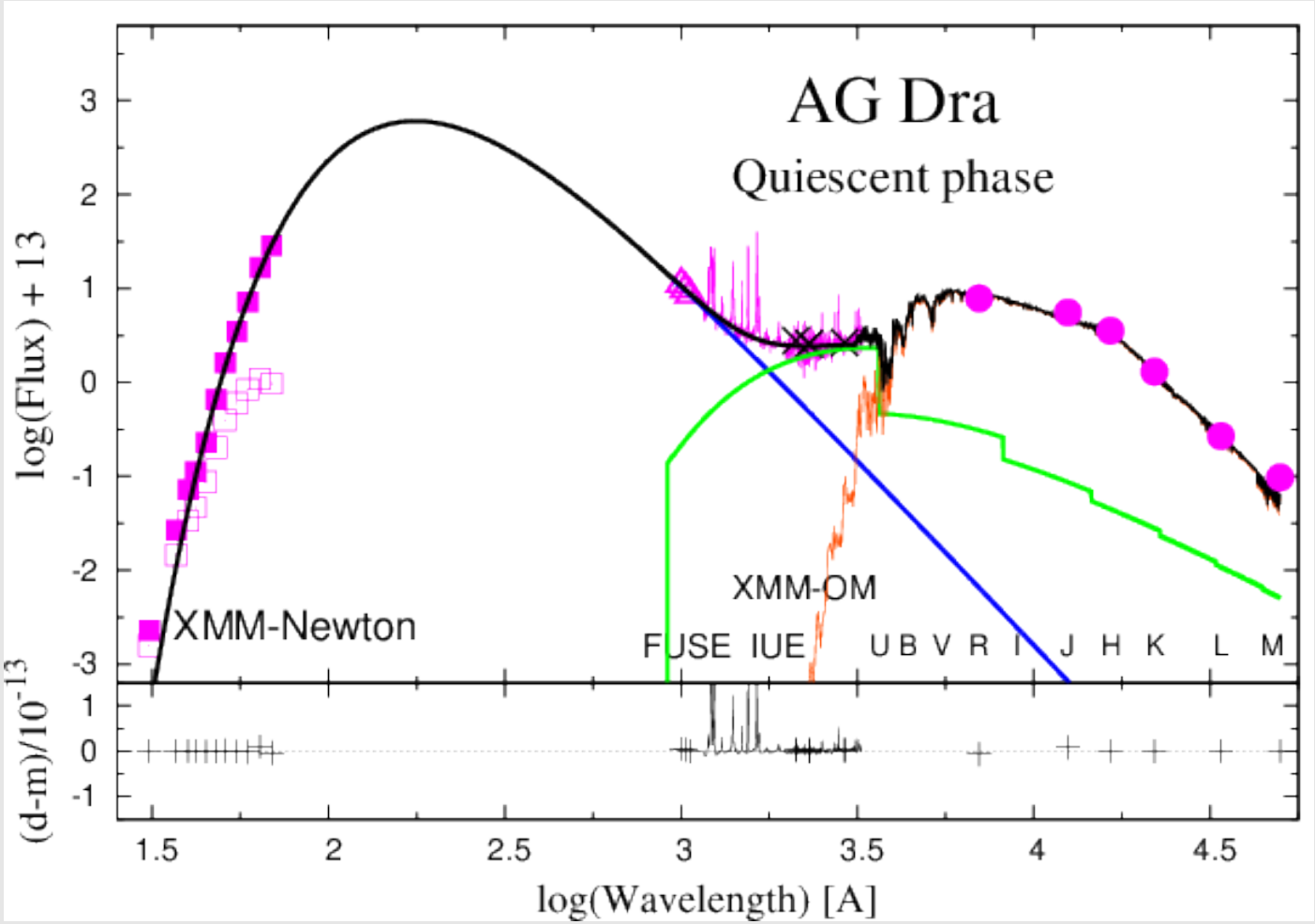

S-type symbiotic star, P_{orb} = 550 d, E_{B-V} < 0.1 mag.

Hot star:

$L_h = 630\,L_{Sun}$

$T_h = 165{,}000\,K$

$R_h = 0.03\,R_{Sun}$

$N_H = 3.13\times10^{20}\,cm^{-2}$

Nebula:

$EM = 1.3\times10^{59}\,cm^{-3}$

$T_e = 21{,}000\,K,$

Giant: K2 III

$L_G = 360\,L_{Sun}$

$T_{eff} = 4300\,K$

$R_G = 33\,R_{Sun}$

Skopal et al. (2009, A&A, 507, 1531)

Symbiotic X-ray binary LIN-358 (in SMC)

P_{orb} is unknown, E_{B-V} = 0.08 mag. d = 60 kpc

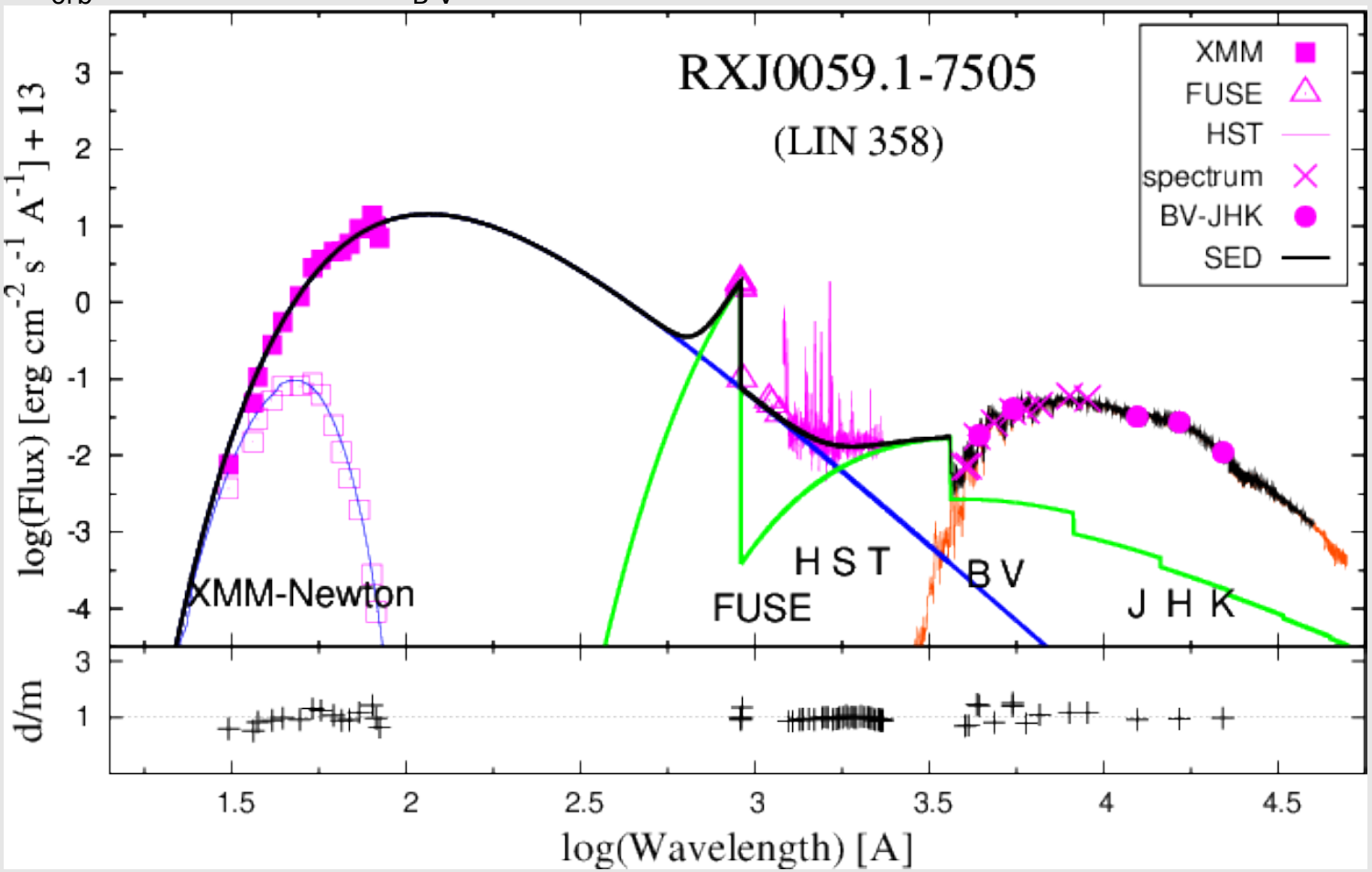

Hot star:

$N_H \sim 6.1 \times 10^{20}\,\mathrm{cm}^{-2}$

$T_h \sim 250{,}000\,\mathrm{K}$

$R_h \sim 0.09\,R_{Sun}$

$L_h \sim 1.1 \times 10^{38}\,\mathrm{erg/s}$

Nebula:

$EM \sim 2.4 \times 10^{60}\,\mathrm{cm}^{-3}$

$T_e \sim 18{,}000\,\mathrm{K}$

Giant:

$T_{eff} = 4000\,\mathrm{K}$

$R_G = 178\,R_{Sun}$

$L_G = 7300\,L_{Sun}$

Fitting parameters: N_H , T_{BB} , angular radius (x d = $R_h \rightarrow L_h$), observed EM, T_e .

Skopal (2015, New Astronomy, 36, 116)

Characteristic parameters (quiescent phase)

Cool component	Hot component	Nebula
$L_G \sim 2000\, L_{Sun}$	$L_h \sim 10^0 - 10^4\, L_{Sun}$ [a)]	$T_e = 1 - 4 \times 10^4\, K$
$T_{eff} \sim 2500 - 4500\, K$	$T_h \sim 1 - 2 \times 10^5\, K$	$EM = 10^{58} - 10^{61}\, cm^{-3}$
$\dot{M}_G \approx 10^{-7}\, M_{Sun}\, yr^{-1}$	$\dot{M}_h \approx 10^{-8} - 10^{-6}$	$\tilde{n} = 10^6 - 10^{12}\, cm^{-3}$

a) – a few times (1 – 10) L_{Sun} for accretion powered systems

a few times 1000 L_{Sun} for nuclear powered systems

Mass-transfer problem in symbiotic binaries

$$L_{WD} \sim a\ few \times 10^3 L_{Sun}\ !$$

The only fuel for this energy is the wind from the RG.

(RG: mass-loss rates ~10^{-8}– 10^{-7} M_{Sun}/year; efficiency: 1-2%: Bondi-Hoyle, 1944)

The long-standing problem:

"How do RGs, well within their Roche lobes, lose sufficient mass to produce the symbiotic phenomenon?"

(Kenyon & Gallagher, 1983)

- What is the mass-loss rate from the RG?
- What is the energy output from the accreting WD ?
- How the wind is transferred onto the WD?

Mass-loss rate from M giants in symbiotic binaries

STB: HI/HII boundary: $X(L_H, p, \dot{M}_W, v_\infty) = f(u, \theta)$; $X = \lim f(u_\infty, \theta) = f(\theta_a)$

$\dot{M}_{wind}$ from the ionized part of the wind (+ X parameter, binary parameters)

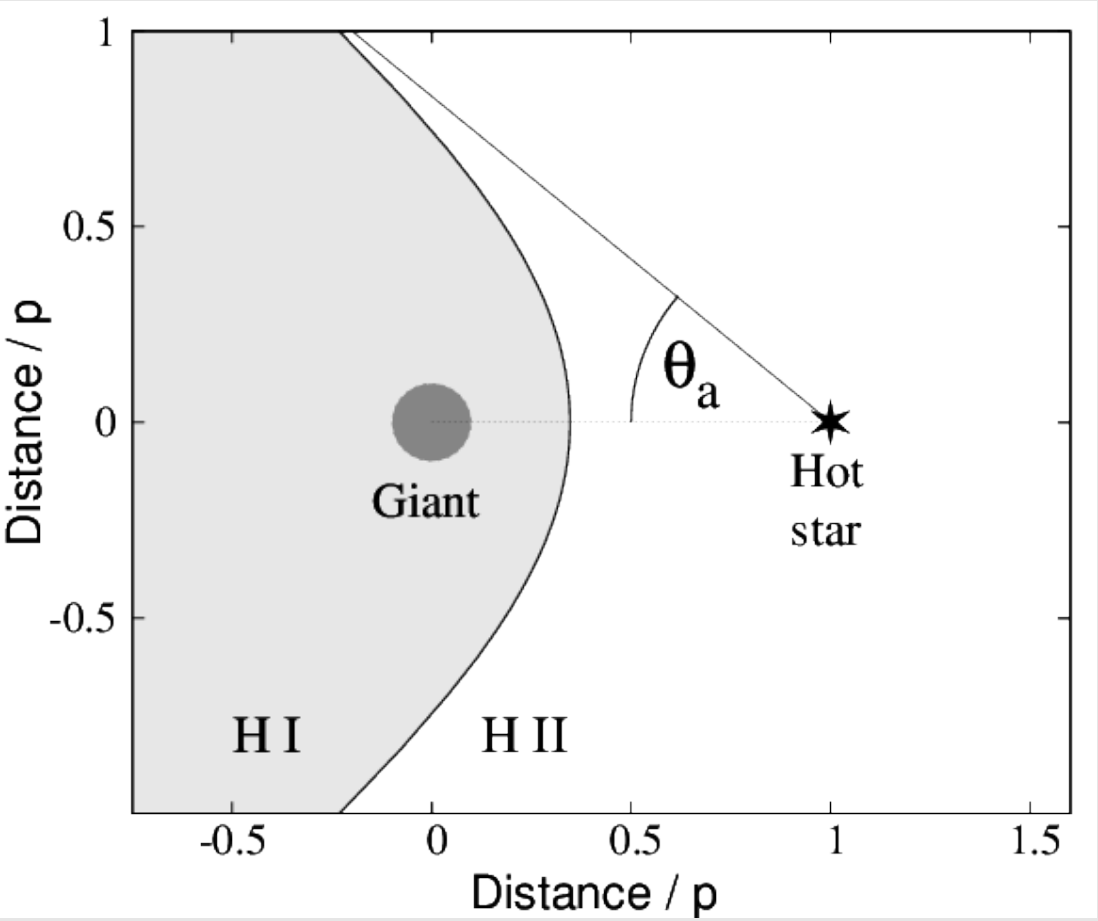

Quiescent phase

neutral wind
from the giant
&
ionizing photons
from the WD

NEBULAR EMISSION

∝

Mass-loss rate

$\dot{M}_{wind}$ from the nebular emission in the UV/optical/near-IR

Emission measure, EM, from model SED

$$EM = \int_{HII} n_p n_e(r)\, dV$$ (V = ionized volume, given by the STB model)

where

$$n(r) = \dot{M}_W / 4\pi r^2 \mu m_H v_w(r)$$

➔ $EM \propto f(\dot{M}_W)$

EM from SED + X from L, T, p

$$\dot{M}_{wind} \sim a\ few \times 10^{-7} M_{Sun}\, yr^{-1}$$

For S-type symbiotic stars

(Muerset et al., 1991, A&A, 248, 458; Skopal, 2005, A&A, 440,995)

$\dot{M}_{wind}$ from the nebular emission in the radio

Uniform mass flow of the ionized wind: $\dot{M}_{wind}/v_{\infty} \propto S_{\nu}$ (Wright & Barlow, 1975)

Seaquist et al. (1993) adjusted the WB formula to the STB model for X=0.5-5
Measuring the flux density at 3.6 cm they obtained:

S-type: dM/dt ~ a few x 10^{-7} Mo/year
D-type: dM/dt ~ a few x 10^{-6} Mo/year

$\dot{M}_{wind}$

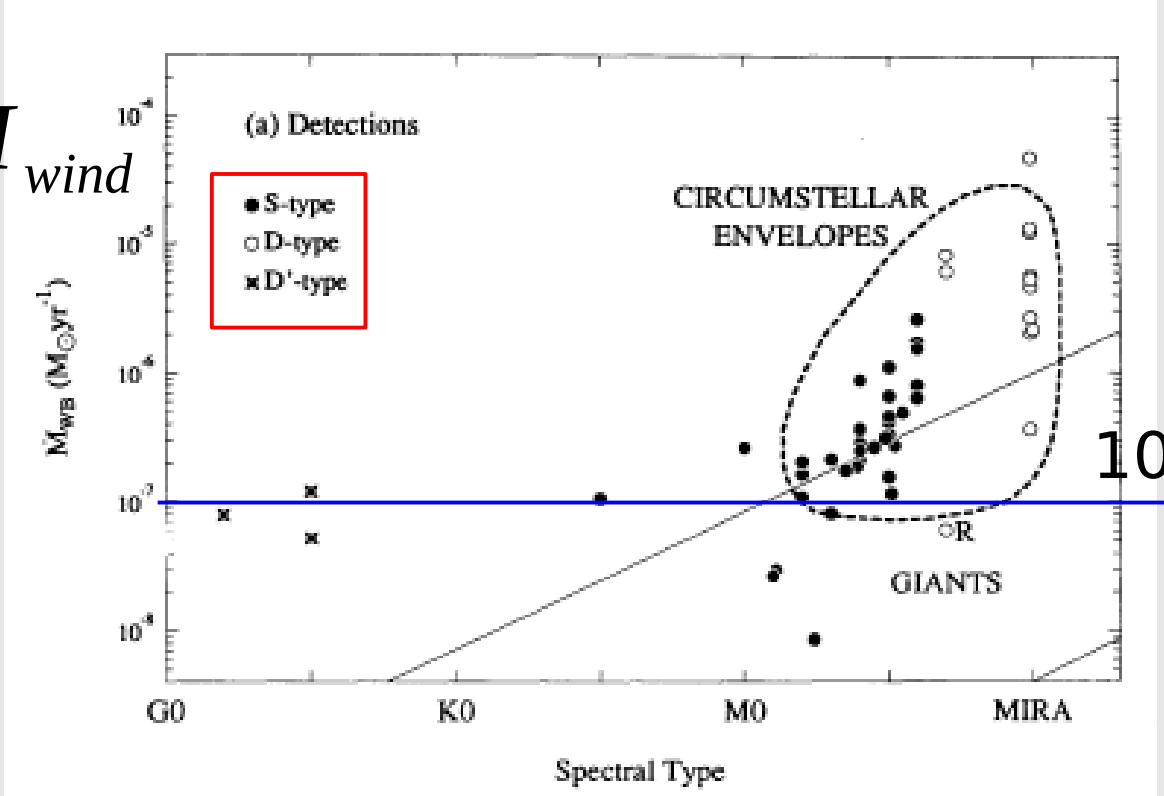

Is the $\dot{M}_{wind} \approx 10^{-7} M_{Sun} / yr$ sufficient to generate L_{WD} ?

What is the accretion rate, $\dot{M}_{acc}$, required to power the WD luminosity, L_{WD} ~ a few x 10^3 $L_\odot$?

What is the mass-transfer ratio, $\mathbf{MTR} = \dot{M}_{acc} / \dot{M}_{wind}$? (i.e. the efficiency)

Standard Bondi-Hoyle wind accretion: MTR ~ a few %

3D simulations: MTR = 0.6 – 10 %, depending on the binary configuration

Is the $\dot{M}_{wind} \approx 10^{-7} M_{Sun}/yr$ sufficient to generate L_{WD} ?

What is the energy output from the accreting WD ?

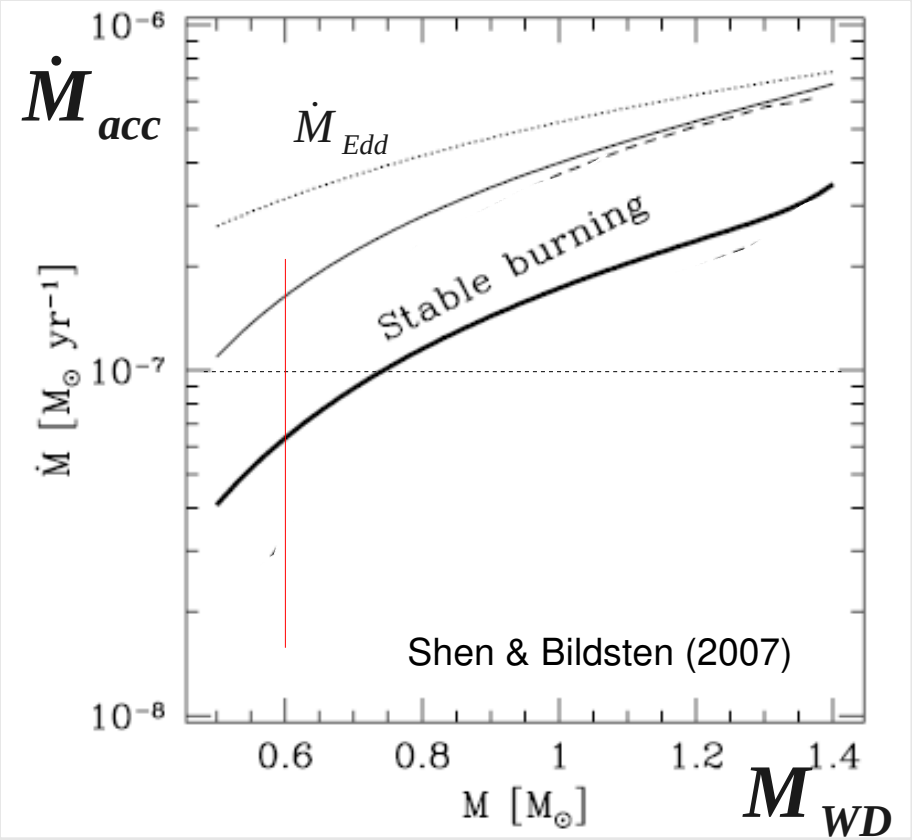

Accretion onto the WD:

L_{acc} + $L_{nuclear}$

$$L_{WD} = \frac{1}{2} G \frac{M_{WD} \dot{M}_{acc}}{R_{WD}} + \eta X \dot{M}_{acc}$$

$$\eta = 6.3 \times 10^{18} \text{ erg/g}, \quad X \equiv 0.7$$

$$M_{WD} \sim 0.6\, M_{Sun}, \quad \dot{M}_{acc} = 10^{-7} M_{Sun}/\text{yr}$$

$$L_{nucl.} \sim \text{a few} \times 10^{3} L_{Sun}$$

$$L_{acc} \sim \text{a few} \times 10^{1} L_{Sun}$$

L_{WD} = a few x10^3 Lo can be achieved by $\dot{M}_{acc} \sim 10^{-7} M_{Sun}/\text{yr}$

but $\dot{M}_{wind} \sim \text{a few} \times 10^{-7} M_{Sun}/\text{yr}$!

How the wind from the giant is transferred onto the WD ?

Gravitationally focused wind accretion in binary systems

The presence of a companion reduces the effective gravity of the mass-losing star in the binary, which leads to the enhancement of the wind mass loss in the orbital plane.

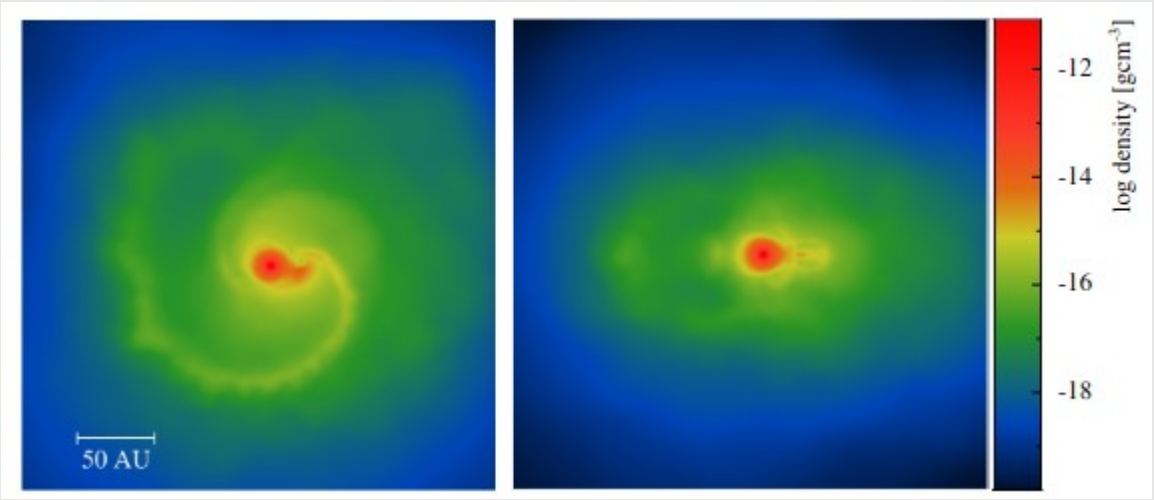

WRLOF: the wind from evolved AGB giant in a D-type SySt is filling the Roche lobe instead of the star itself:
(Mohamed & Podsiadlowski, 2012)

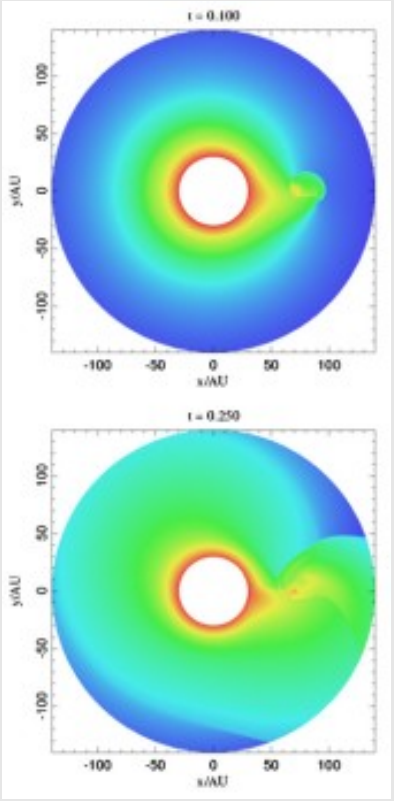

Density contours in a binary with a = 70 AU. White circle is the wind acceleratiion zone.
Mass-transfer rate ~ 20-50% larger than BHL approximation.
(de val-Borro et al. 2009, 2017.)

Tout & Eggleton 1988, MNRAS, 231, 823
Frankowski & Tylenda, 2001, A&A, 367, 513
Booth et al. 2016, MNRAS, 457, 822
El Mellah et al. 2020, A&A, 637, A91

Focusing by the Wind Roche-Lobe Overflow (WRLOF) for Mira-type symbiotic binaries

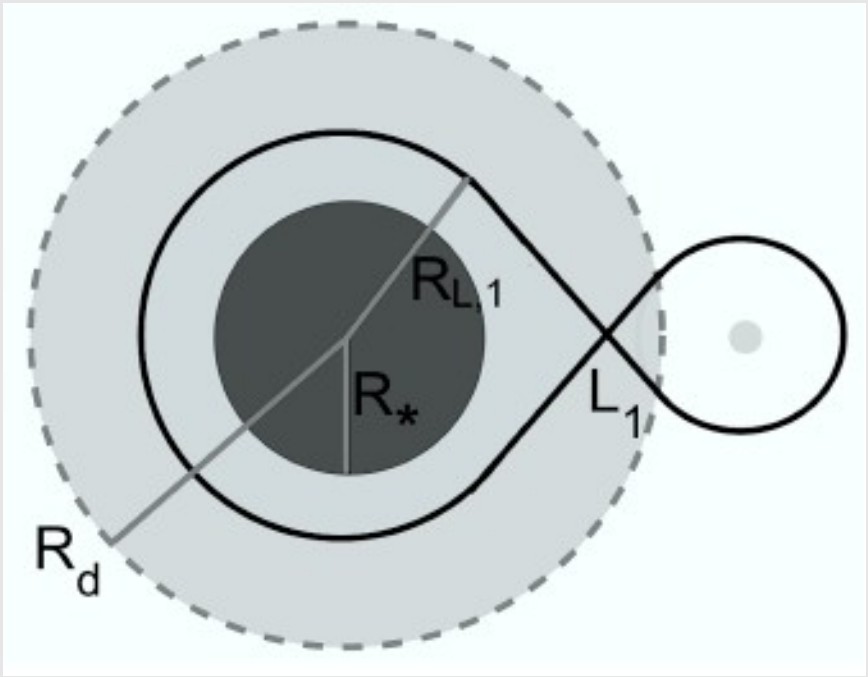

WRLOF can occur in systems where a slow wind within the acceleration zone (R_d , gray area) lies close to R_L

$$v_\infty \sim 5-10\,\mathrm{km/s}$$

Figure from Abate et al. (2013)

Mohamed & Podsiadlowski (2007, 2012)
A new mass transfer mode in Mira-type binaries (D-type SySts)

WRLOF: The wind is filling the R_L instead of the star itself

Material is gravitationally confined to the R_L and falls into the potential of the accretor via the L_1 point.

The wind of the evolved star is focused towards the orbital plane.

WRLOF mass transfer ratio
~
10 x Bondi-Hoyle values

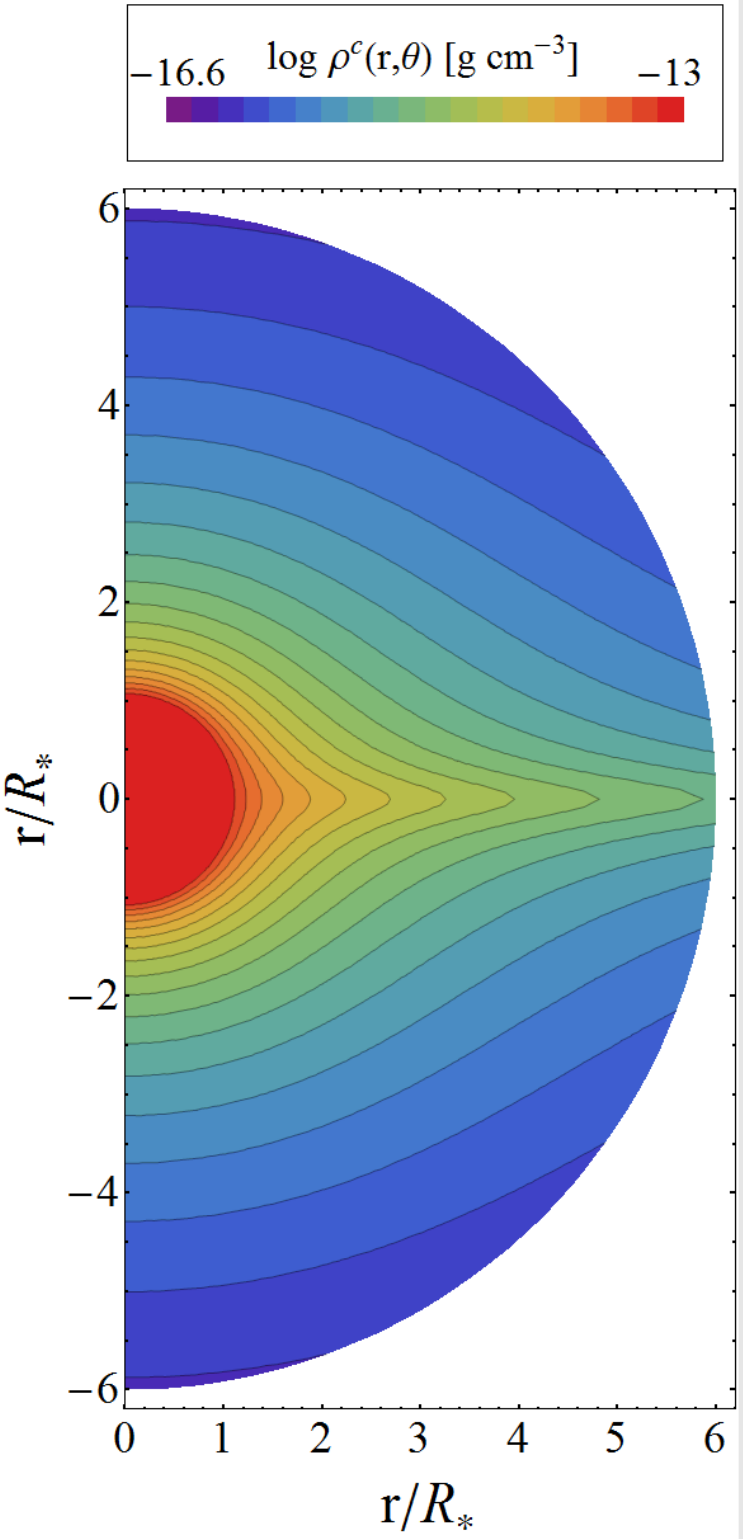

Focusing by the wind compression model

Wind is compressed due to the rotation of the star.
The model was elaborated by
Bjorkman & Cassinelli 1993, ApJ, 409, 429.

Mass continuity equation:

$$\rho^c(r,\theta) = \frac{\dot{M}}{4\pi r^2 v_r(r)}\left(\frac{d\mu}{d\mu_0}\right)^{-1}$$

$\dot{M}$ – total mass-loss rate from the star

$(d\mu/d\mu_0)^{-1}$ – describes the compression of the wind

Giants in S-type symbiotic stars rotate:

$v_{rot}\sin(i) \sim 6 - 9.5$ km/s

(e.g. Zamanov et al., 2008)

Figure: Density distribution in the wind compr. model:

$\dot{M} = 10^{-7} M_{Sun}\, yr^{-1}$, $R_G = 100_{Sun}$,

$v_{rot} = 6$ km/s, $v_\infty = 20$ km/s, $f(r=6,\pi/2) = 5.4$

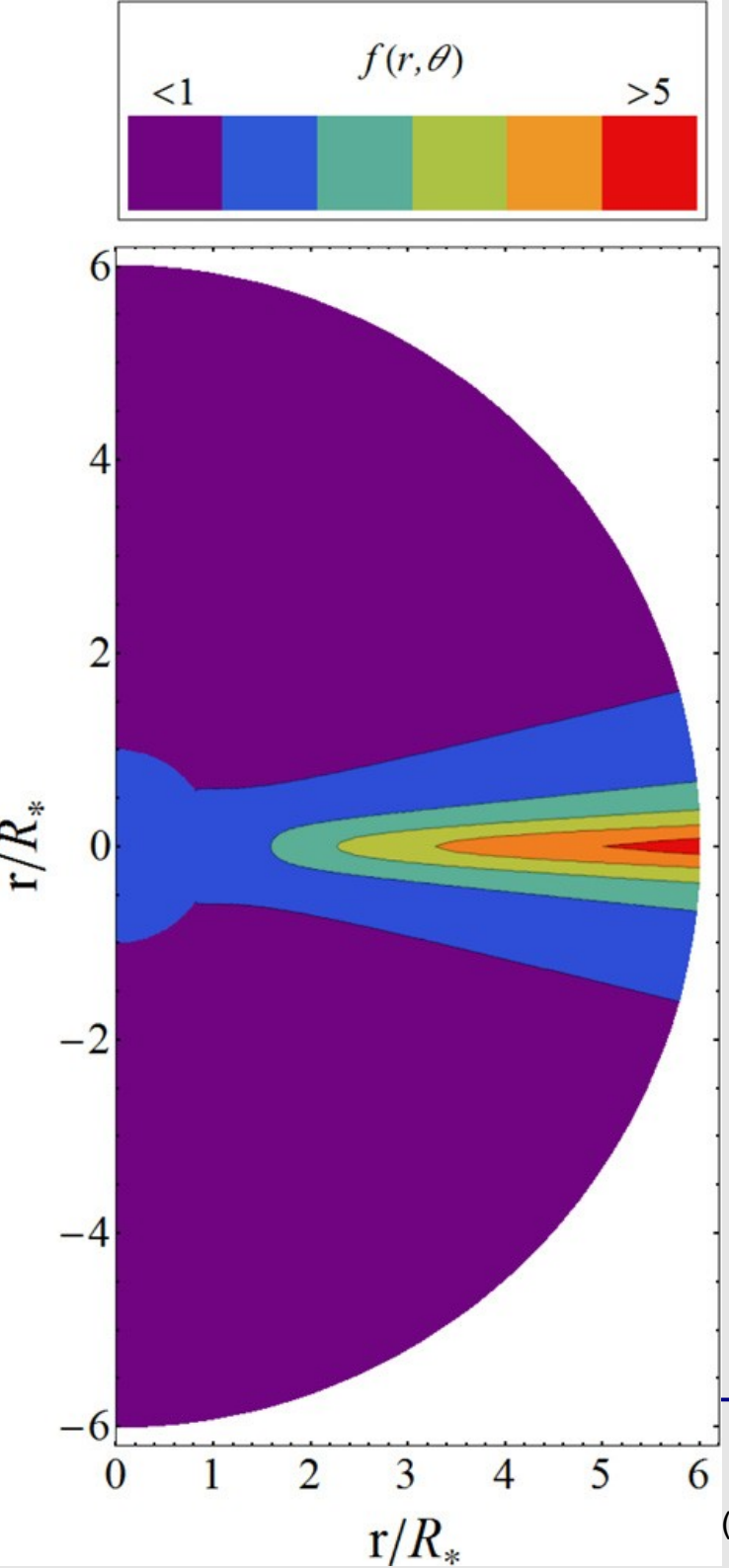

Focusing by the wind compression model

Mass-loss ratio (to compare $\dot{M}$ and $\dot{M}(r,\theta)$):

$$f(r,\theta) = \frac{\dot{M}^c(r,\theta)}{\dot{M}} = \frac{\rho^c(r,\theta)}{\rho^{sph}(r)} = \left(\frac{d\mu}{d\mu_0}\right)^{-1}$$

$\dot{M}^c(r,\theta)$ is given by the local density, $\rho^c(r,\theta)$

$\dot{M}$ is the total mass-loss rate

Accretion rate:

$$\dot{M}_{acc} \approx \eta \times f \times \dot{M}$$

$\eta \sim$ a few $\times 0.01$ (B-H efficiency)

$f \sim 5-15$

Figure: Mass-loss ratio f(r,theta):

$\dot{M} = 10^{-7} M_{Sun}\, yr^{-1}$, $R_G = 100_{Sun}$,

$v_{rot} = 6$ km/s, $v_\infty = 20$ km/s → $f(r=6, \theta=\pi/2) = 5.4$

(Skopal & Carikova, 2015, A&A, 573, A8)

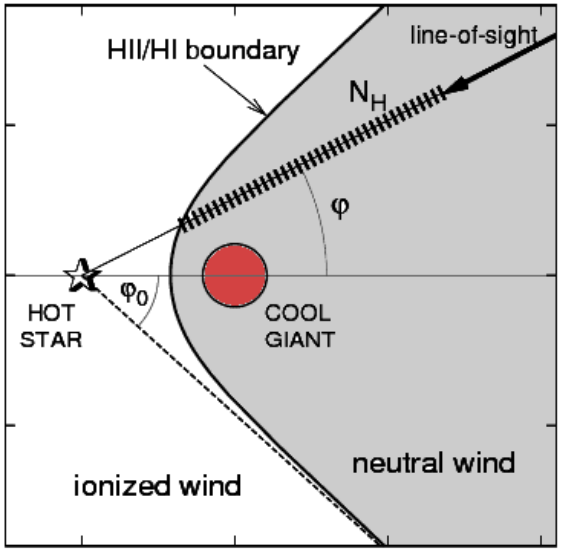

Observational indication of the wind focusing

In eclipsing systems: EG And and SY Mus

Rayleigh scattering:

$$F_\lambda(\varphi) = F_\lambda^0 \exp\left[-n_{H0}^{obs}(\varphi)\sigma_{Ray}(\lambda)\right]$$

From the continuity equation:

$$n_{H0}(\varphi) = \frac{\dot{M}}{4\pi\mu m_H}\int_{-\infty}^{l\varphi}\frac{dl}{r^2 v(r)} \quad \text{to } H^0/H^+$$

Spherical equivalent of the mass-loss rate (n_H from theorbital plane):

$$\dot{M}_{sp} \sim \text{a few} \times 10^{-6} M_{Sun}\, yr^{-1}$$

→ enhanced wind at the orbital plane: ↑ $\dot{M}_{acc}$

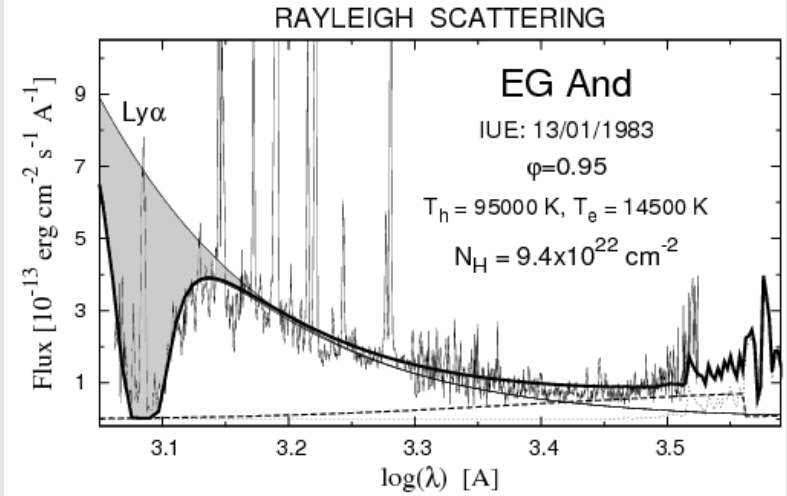

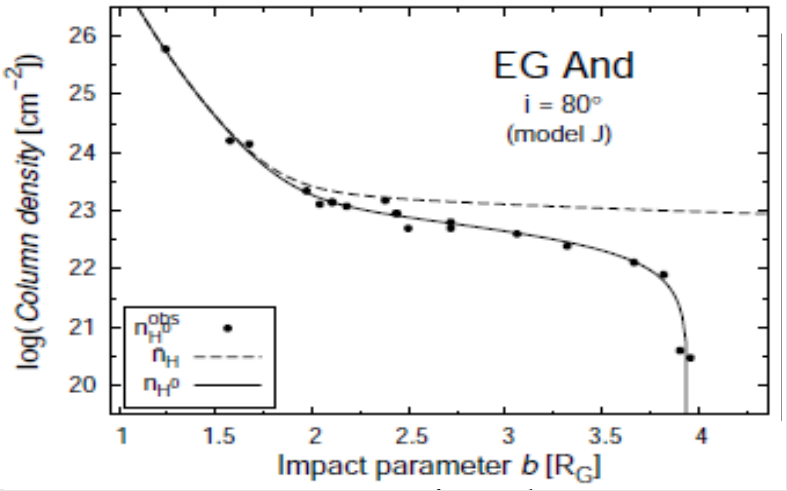

Shagatova et al. 2016, A&A, 588,A83
Shagatova 2017, PASP, 129, 067001

Wind focusing in EG And from the nebular [OIII] λ5007 line

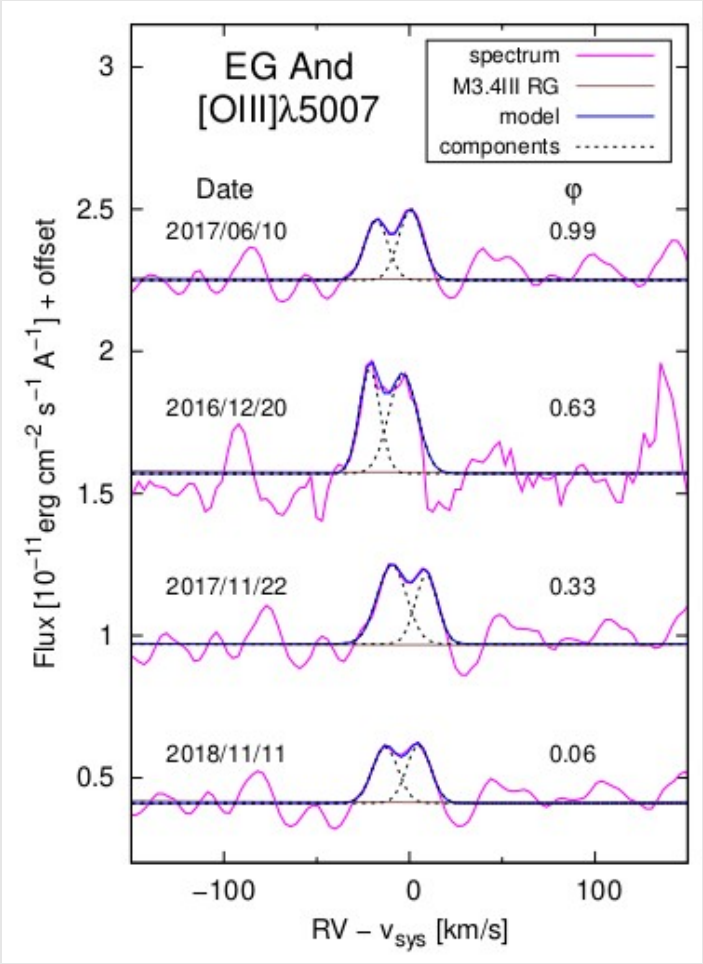

The nebular [OIII]λ5007 line is splitted into two components on the high-resolution spectra (R~35000).

Top: RVs of [OIII]λ5007 line from medium-resolution spectra are not splitted, they are shifted by -9 km/s from the RG motion (orange line).

Middle: RVs of blue and red components of the profile from the high-resolution spectra. Both components follow the RG orbital motion, being shifted by -15 and +3 km/s (dashed lines).

Bottom: Sketch of [OIII] line zones in the vicinity of the RG at/around its polar regions.

This startling properties of the nebular [OIII] line provides an independent indication of the wind focusing towards the orbital plane – the key to understanding the efficient wind mass transfer in symbiotic binary stars.

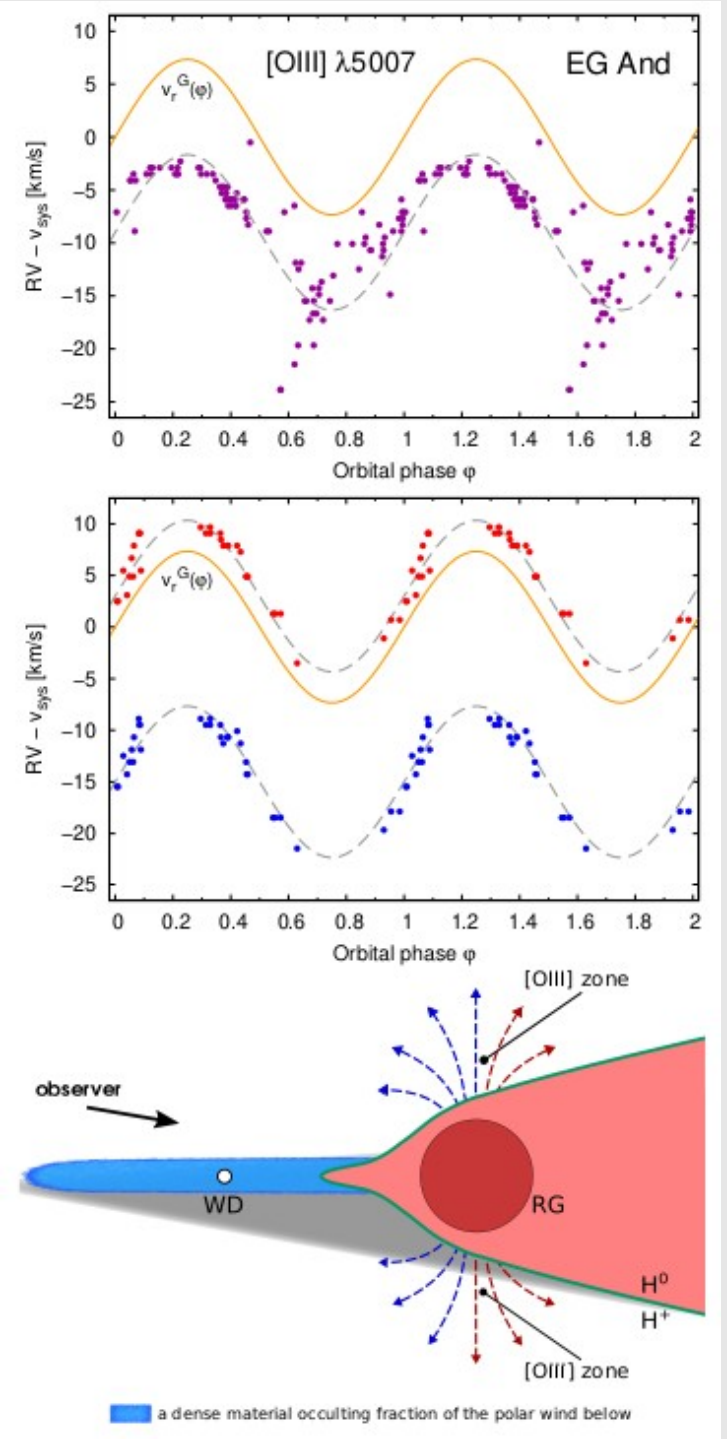

Shagatova et al., 2021, A&A, 646, A116

Thermonuclear outbursts on the white dwarf surface in symbiotic stars

– Nova outbursts: (recurrent) symbiotic novae

– Z And-type outbursts in symbiotic stars

A white dwarf's response to mass accretion

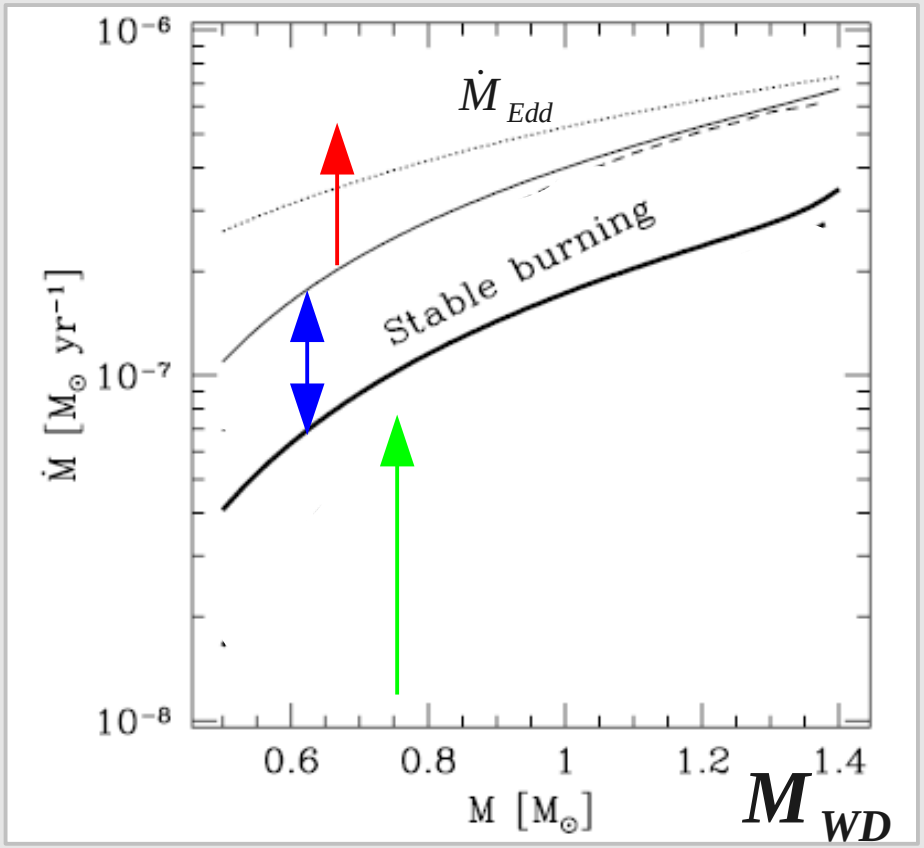

Shen & Bildsten 2007, ApJ, 660, 1444;
Nomoto et al. 2007, ApJ, 663:1269;
Wolf et al. 2013, 777:136

Accreting WD increases its mass:

(i) at low rates up to $\Delta M \rightarrow P_{crit}$:
ignition of a nova outburst

(ii) at high rates of ~10^{-7} M_{Sun}/year:
stable H-burning in a shell

(iii) if rates >~10^{-7} M_{Sun} /year:
Z And-type outbursts

(e.g., Paczynski & Zytkow 1978, ApJ, 222, 604; Yaron, et al., 2005, ApJ, 623, 398; Hachisu et al., 1996, ApJ, 470:L97; Skopal et al. 2017, A&A, 604, A48)

$$L_{WD} = L_{acc.} + L_{nucl.} = G\frac{M_{WD}\dot{M}_{acc}}{R_{WD}} + \eta X \dot{M}_{acc} \quad (\eta = 6.3\times10^{18}\,\mathrm{erg/g},\ X \equiv 0.7)$$

Generated energy: ~ L_{WD} + energy to lift off ΔM_{wind}

I.
Observational manifestations of mass accretion onto white dwarfs in symbiotic stars

1. $\dot{M}_{acc} < \dot{M}_{stable}$ + $P_b < P_{crit}$: ***Accretion – powered*** (accreting-only) SySts
(e.g., EG And, SU Lyn, CQ Dra, hidden SySts)

Weak or no activity in the optical, but a strong excess and variability in the UV—X-rays.
(e.g., Skopal, A. 2005, ASP Conf. Ser. 330, 463; Munari et al. 2021, MNRAS, 505, 6121; Perko, M. 2024, CoSka, 54, 75)

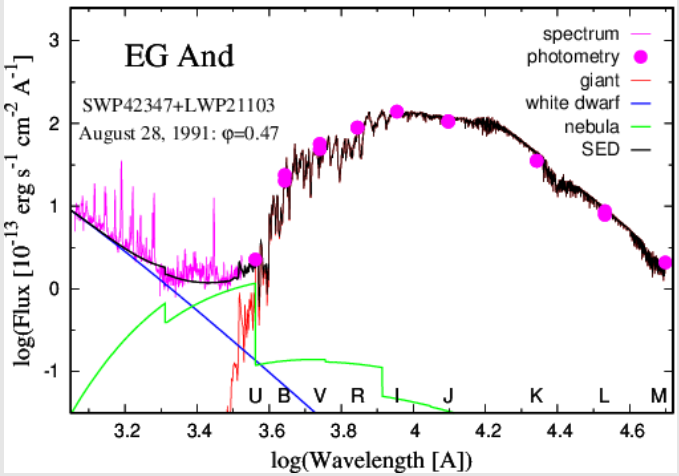

M3III + WD, $P_{orb} = 482\,\mathrm{d}$, eclipses,
$L \sim 2.5\times10^{35}\left(d/590\,\mathrm{pc}\right)^2$ erg/s,
orbital-related var. of the opt. em. l.

Vogel, M. 1991, A&A, 249,173;
– 1992, A&A, 260, 156;
Kenyon & Garcia, 2016, AJ, 152, 1;
Shagatova et al. 2016, A&A, 588, A83;
– 2021, A&A, 646, A116.

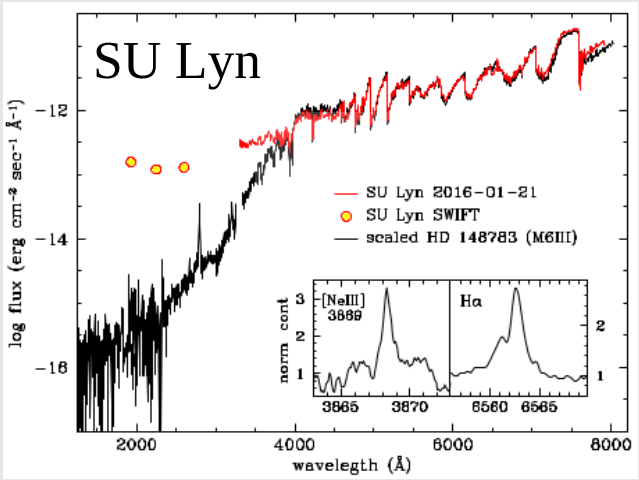

M5.8III + WD, variable UV,
$L_{UV} \sim 1\times10^{34}\left(d/640\,\mathrm{pc}\right)^2$ erg/s,
variable opt. emission lines.

Mukai et al. 2016, MNRAS, 461, L1;
Lopes de Oliveira et al. 2018, ApJ, 864:46;
Kumar et al. 2021, MNRAS, 500, L12
Ilkiewicz et al. 2022, MNRAS, 510, 2707

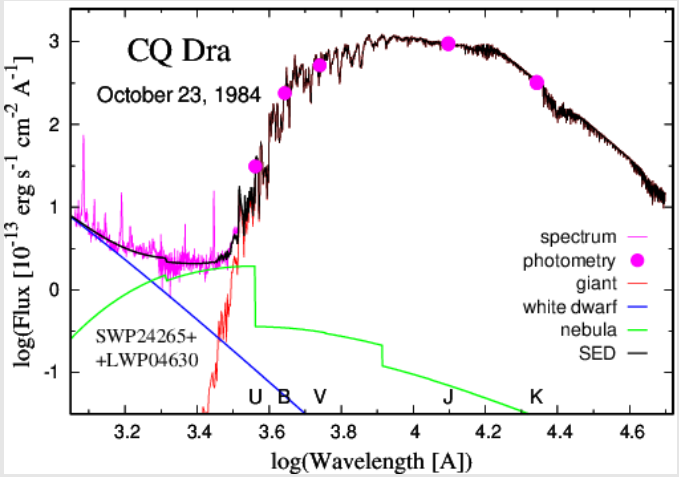

M3III + WD, $P_{orb} = 1703\,\mathrm{d}$,
$L \sim 2.5\times10^{34}\left(d/178\,\mathrm{pc}\right)^2$ erg/s,
variable nebular continuum.

Reimers, D. 1985, A&A, 142, L16;
Wheatley et al. 2003, MNRAS, 346, 855;
Skopal, A. 2005, ASP Conf. Ser. 330, 463;
– 2005, A&A, 440, 995;

2. $\dot{M}_{acc} < \dot{M}_{stable}$ + $P_b = P_{crit}$ → ***nova outbursts*****:** (recurrent) symbiotic novae.

(a) Post-outburst evolution at $\dot{M}_{acc} < \dot{M}_{stable}$: usually, recurrent SyNe with ↑M_{WD}.

RS Oph: K7III + WD, P_{orb} = 455 d, P_{rec} ~ 15-20 years; Figure: Visual LC from AAVSO

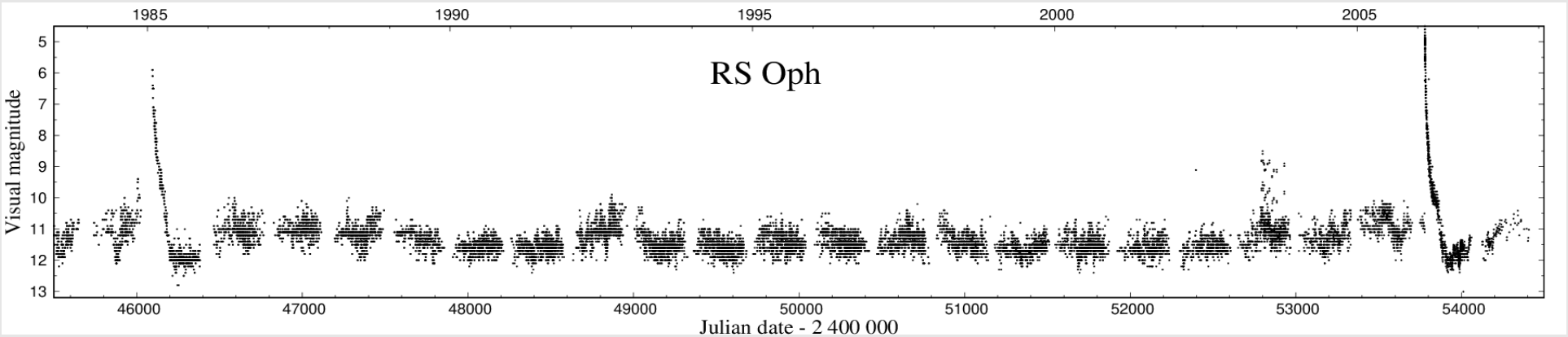

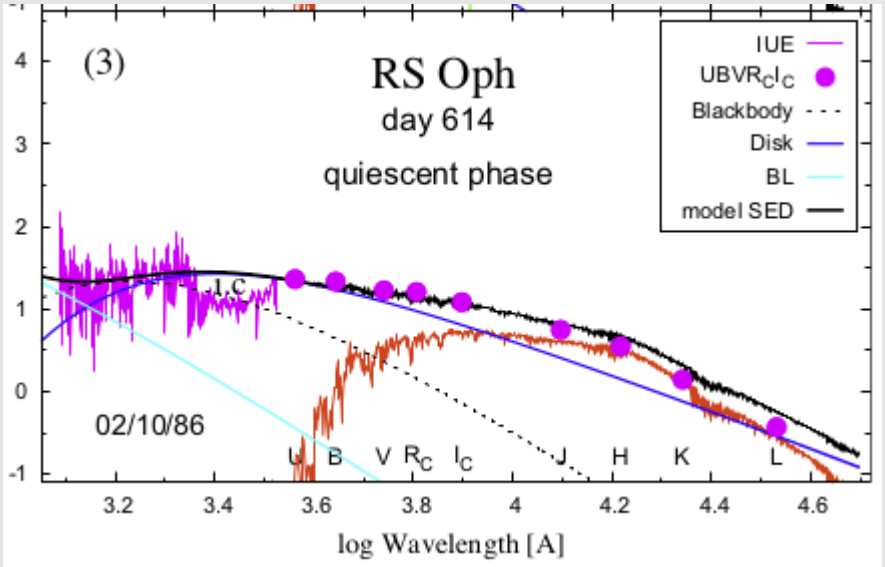

Model SED for RS Oph during quiescence.
dM/dt ~ 5 x 10^{-8} M_{sun}/yr, L_{AD} ~ 360 L_{sun}

(Skopal, 2015, NewA, 34, 123)

T CrB: M4III + WD, P_{orb} = 228 d, P_{rec} ~ 80 yr

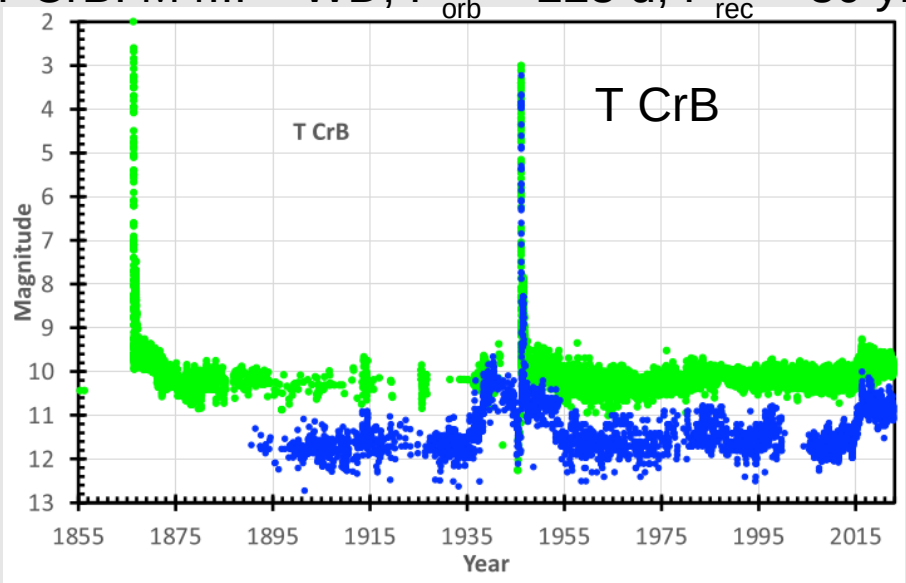

V (green) and B (blue) light curves of T CrB covering eruptions in 1866 and 1946.

(Schaefer, 2023, MNRAS, 524, 3146)

(b) Post-outburst evolution at $\dot{M}_{acc} \sim \dot{M}_{stable}$: ***Nuclear – powered*** (shell-burning) SySts: L = a few x $10^3 L_{Sun}$, wave-like orbital-related variability (if known, M_{WD}<1 M_{Sun}).

PU Vul:
M6III + WD
P_{orb} = 4897 d
Post-outburst:
EM ~ 10^{60} cm^{-3}
L_{WD} ~ 3000 L_{solar}
(Tatarnikova et al., 2018; Muerset & Nussbaumer, 1994; Cuneo et al. 2018)

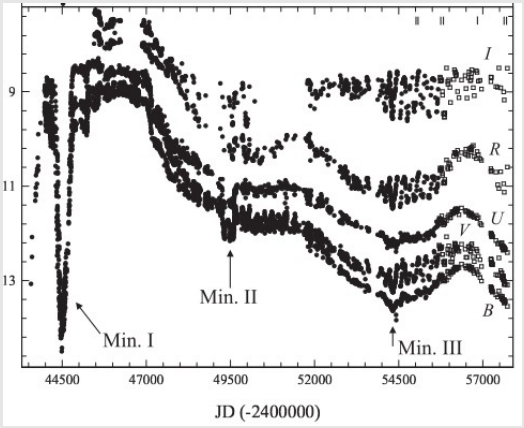

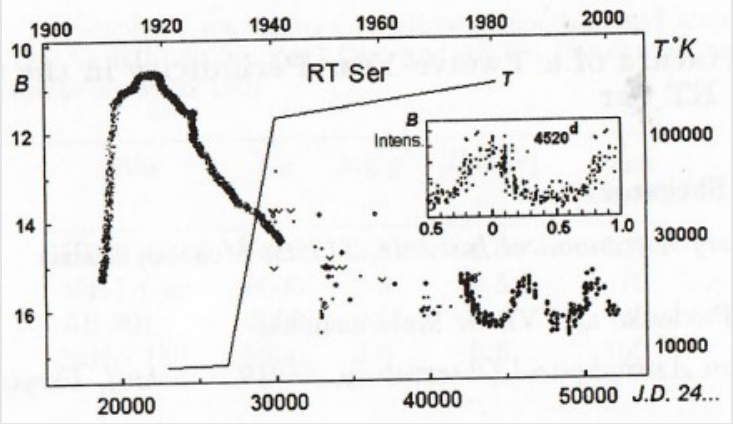

RT Ser:
M5.5III + WD
P_{orb} = 4431 d
Post-outburst:
L_{WD} ~ 3300 L_{solar}
(Shugarov et al. 2003; Muerset & Nussbaumer, 1994)

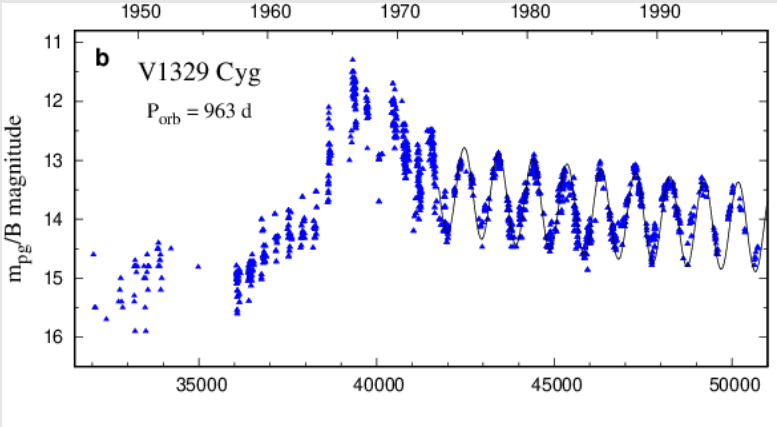

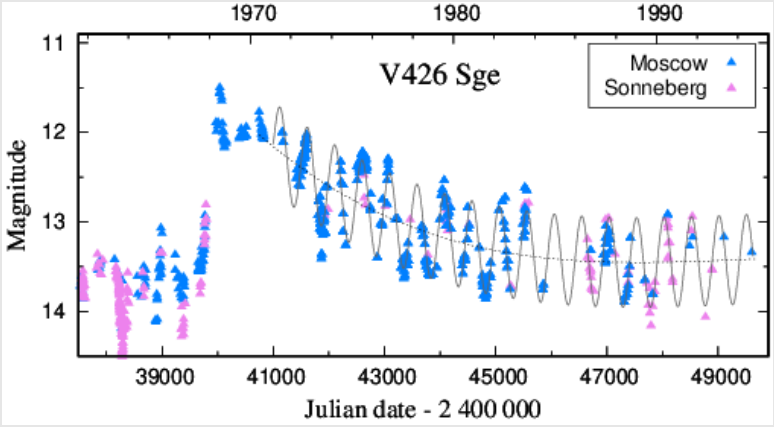

V1329 Cyg: M6III + WD, P_{orb} = 960 d, Nova outburst in 1964; eclipsing; Post-outburst: L_{WD} ~ 7000 L_{solar}, EM ~ 10^{60} cm^{-3} , T_{BB} ~ 170 kK, R_{WD} ~ 0.1 R_{solar}.

(Munari et al. 1988, A&A, 202, 83; Muerset & Nussbaumer, 1994, A&A, 282, 586; Schild & Schmid, 1997, A&A, 324, 606; Skopal, A. 2005, A&A, 440, 995)

V426 Sge: M4.8III + WD, P_{orb} = 494 d, Nova outburst in 1968, non-eclipsing, Post-outburst: L_{WD} ~ 2000 L_{solar}, EM ~ $10^{59\text{-}60}$ cm^{-3} , T_{BB} ~ 150 kK, R_{WD} ~ 0.07 R_{solar}.

(Adapted according to Skopal et al. 2020, A&A, 636, A77)

3. $\dot{M}_{acc} > \dot{M}_{stable}$: **Z And – *type* *outbursts*** due to a transient increase in $\dot{M}_{acc}$.

(Theoretical predictions support this interpretation)

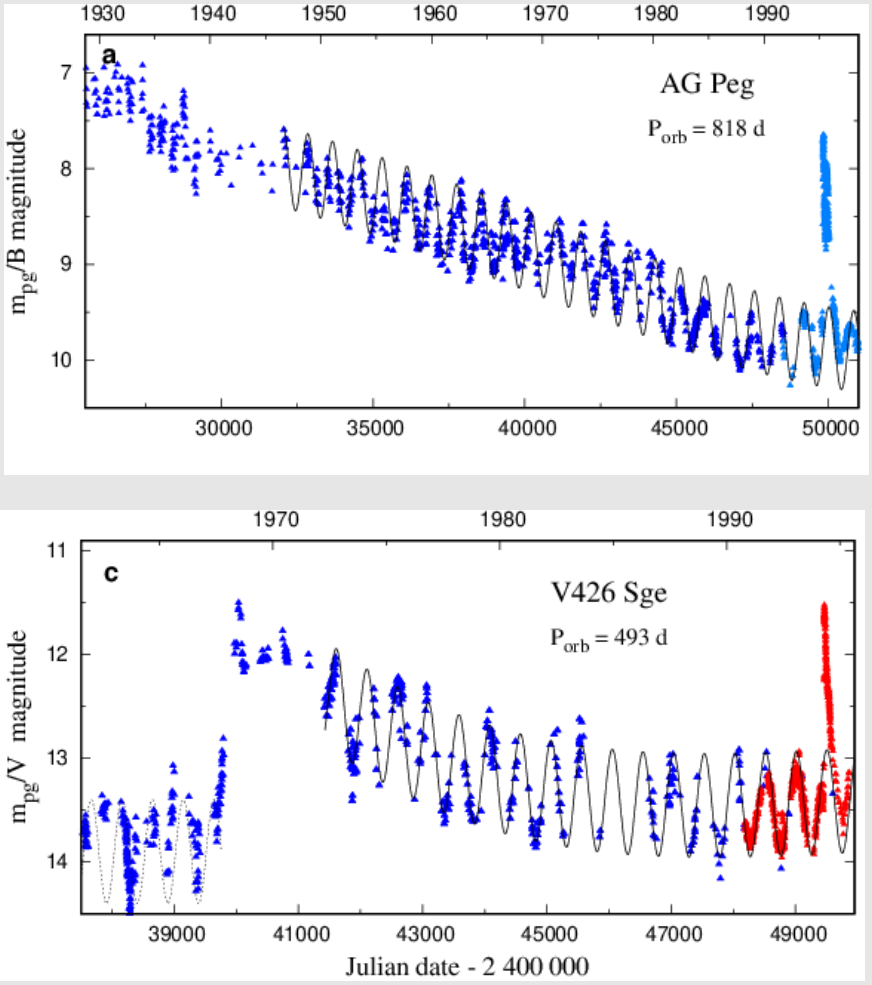

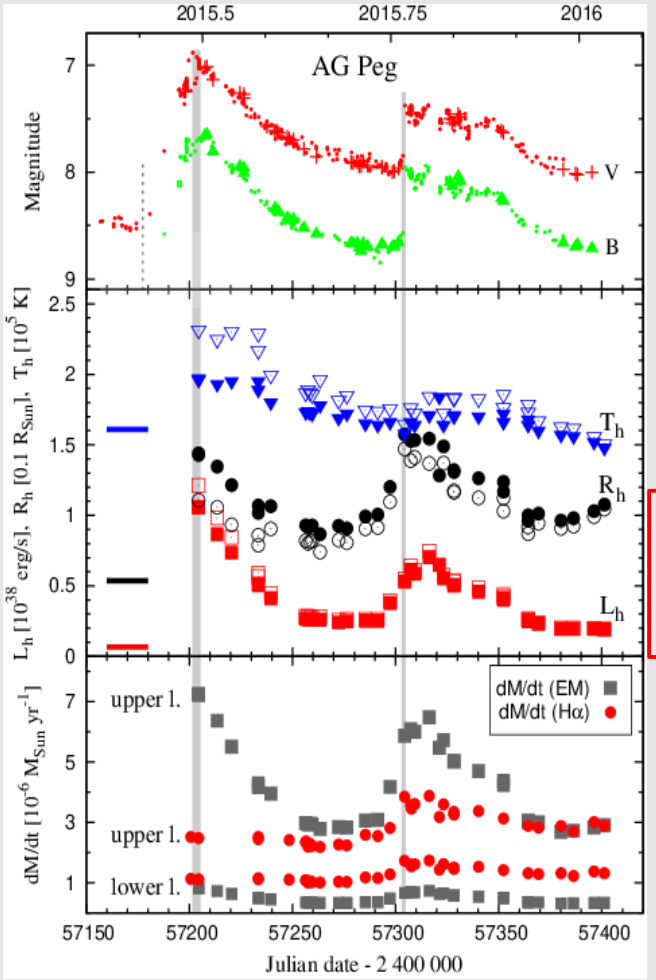

If $\dot{M}_{acc} \succ \dot{M}_{stable}$,

optically thick **wind blows** from the WD at

$$\dot{M}_{wind} \gtrsim 10^{-6}\, M_{sun}/\,year$$

and

$$L_{WD} \sim 10^{37-38}\, erg/\,s$$

(see, Hachisu et al. 1996).

These parameter values are determined during Z And-type outbursts (here AG Peg).

What ignites the outburst?

(i) A disruption of the AD → infall of H-rich material onto the WD.

(ii) Variation in the mass-transfer from the red giant.

Figure. *Left:* Transition from the symbiotic nova outburst to quiescence and to Z And-type outburst for AG Peg (top) and V426 Sge (bottom). *Right:* LC and L, R, T, and dM/dt parameters for AG Peg during its 2015 outburst (Skopal et al. 2017, 2020).

(Sokoloski et al. 2006; Bisikalo et al. 2006)

Enhanced wind mass-loss rate during outbursts

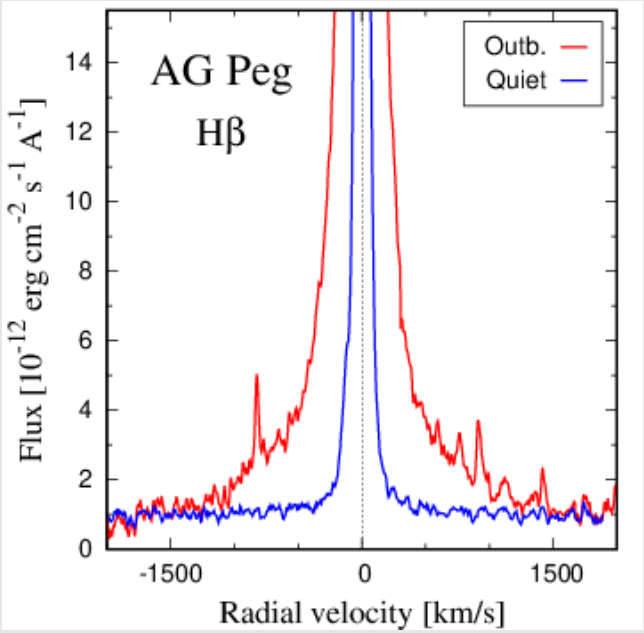

During Z And-type outbursts a strong wind blows at rates of

a few x 10^{-6} M_{sun}/year

From modelling *EM* or *line profiles*

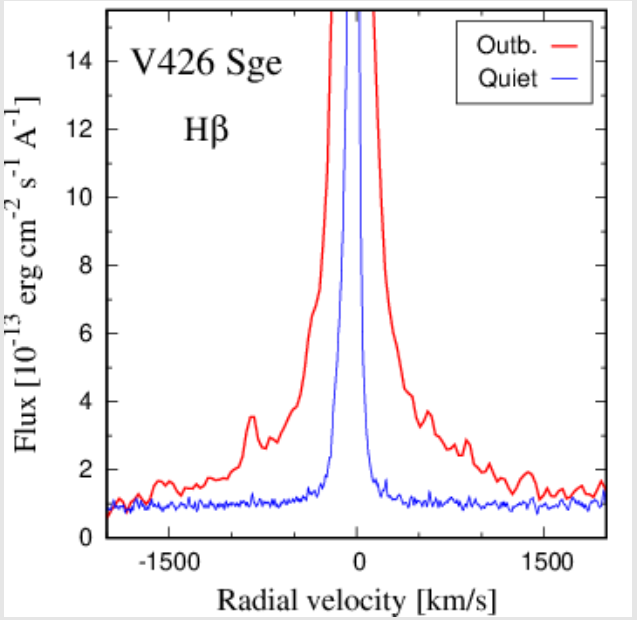

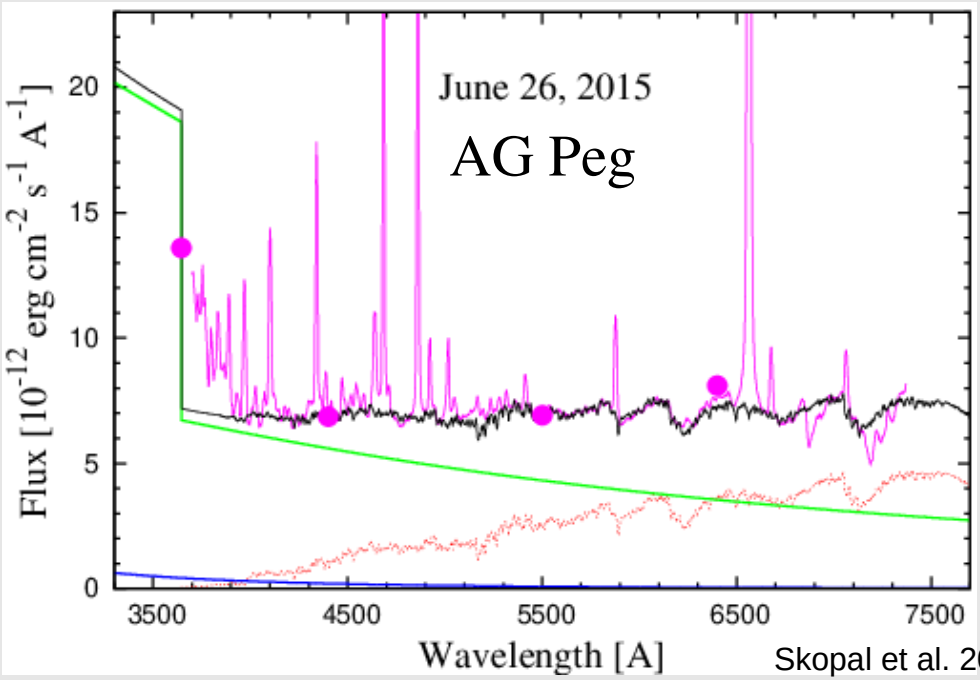

Active phase: Nebular emission is generated by the ionized wind from the burning WD. Its emission measure, EM, is

$$EM \propto \left(\frac{\dot{M}_{WD}}{v_\infty}\right)^2$$

$$\mathrm{EM} \sim (2-7)\times 10^{60}\ \mathrm{cm}^{-3}$$
$$v_\infty \sim 1200\ \mathrm{km/s}$$
$$\dot{M} \sim (1-5)\times 10^{-6}\ \mathrm{M}_{Sun}\mathrm{yr}^{-1}$$

Skopal et al. 2017, 2020

Collimated ejections (jets) during outbursts of symbiotic binaries

Detection of collimated ejection from white dwarfs (WD) in symbiotic binaries is very rare and has employed a variety of methods in X-ray, radio, optical imagery, and spectroscopy. To date, its signature in the optical spectra has only been recorded for *six objects* (MWC 560, Hen 3-1341, StHα 190, Z And, BF Cyg and St 2-22). They represent very exciting events.

A common element in all jet-producing systems is the *central accreting star*, which implies that their *accretion disks play an important role* in the formation of this type of mass outflow (e.g., Livio 1997, 2004).

The nature of this phenomenon is not yet understood well.

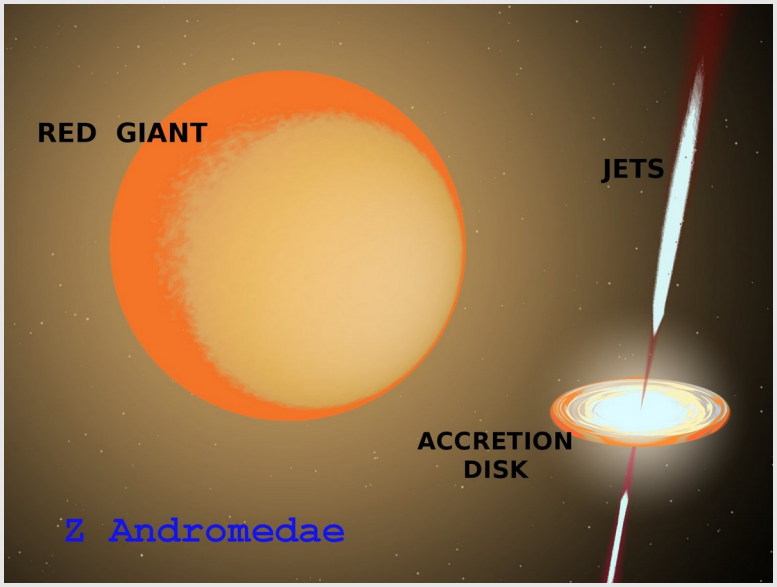

The jet ejections by the symbiotic star MWC 560 (pole-on system; i~0)

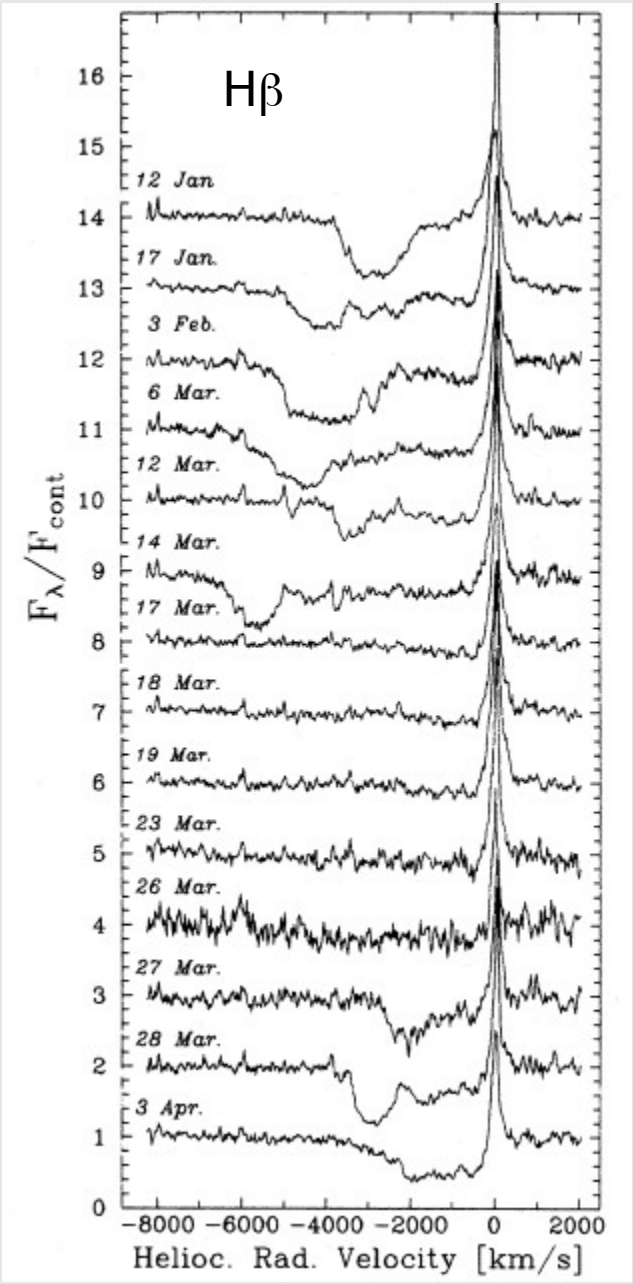

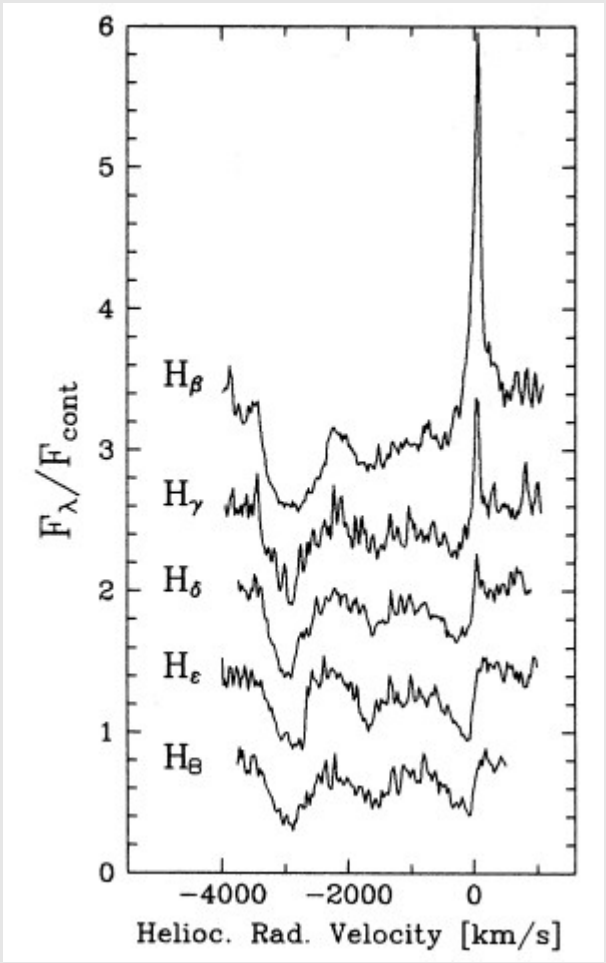

The evidence and time variations

Time-scale: days – weeks

V_{jet} ~ 2000 – 6000 km/s

Tomov et al. 1992; Schmid et al. 2001

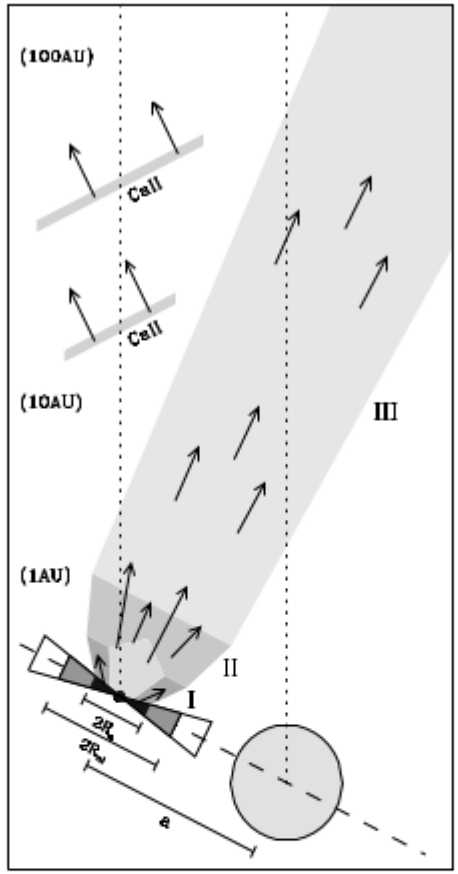

Fig. 19. Schematic geometry of the MWC 560 outflow and the location of the line of sights (dotted lines) to the continuum source and to the red giant. The outflow is divided into three jet regions I, II and III according to the properties of the corresponding absorption components. For illustration purposes the different components are not drawn to scale (see approximate distances along the jet indicated on the left) and the inclination of the jet (or orbital plane) is too large. In particular the line of sight from the accreting object should pass for a longer distance through jet region III. Geometric dimensions for the continuum source $2R_c$, the narrow line region $2R_{nl}$ and the binary separation a are indicated.

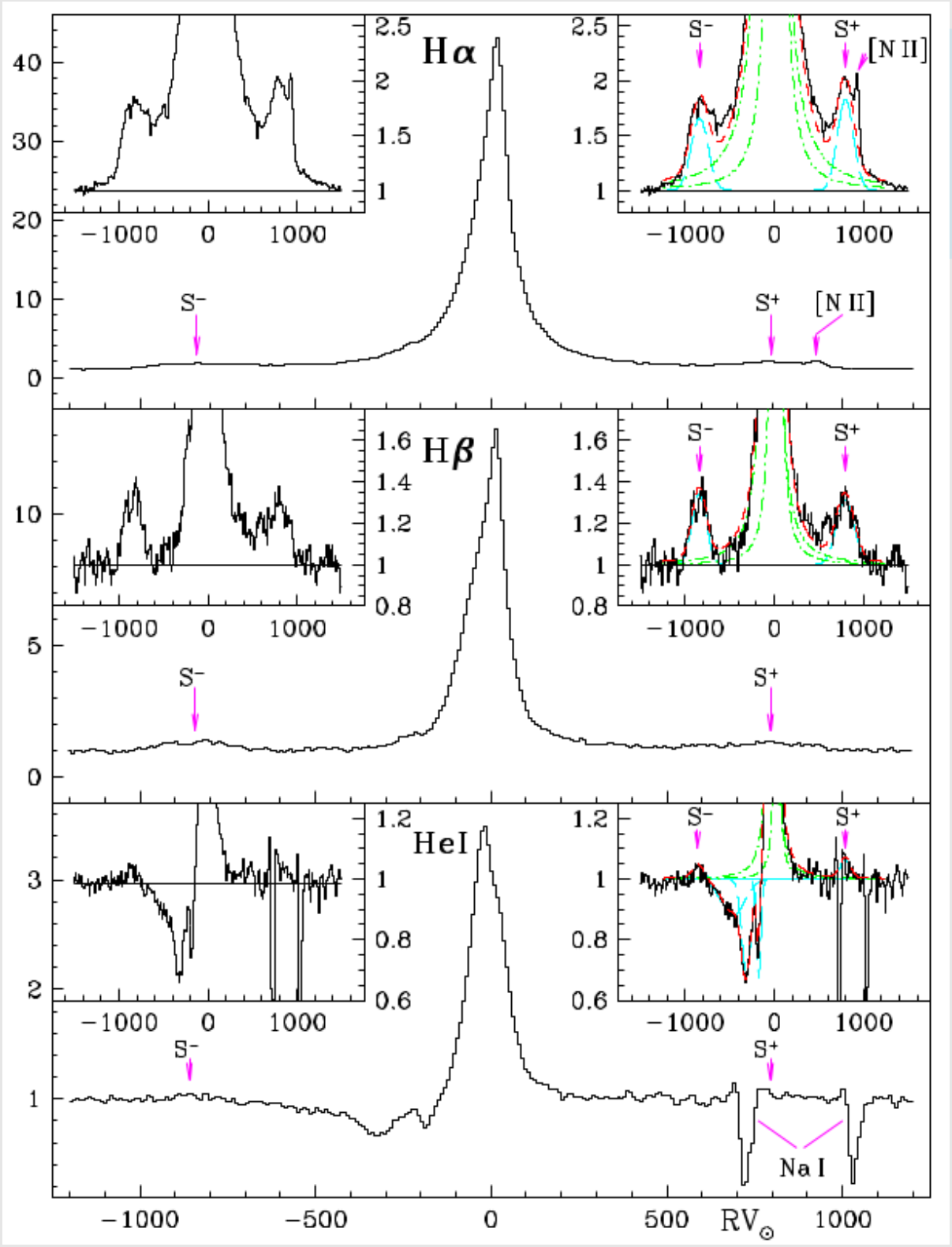

The jet ejections by systems with i~50 – 80° satellite components to main emission core

Hen3-1341

Collimated ejection: Hα, Hβ, HeI

The jets are indicated as emission components at +/- 820 km/s on both sides of the main emission line.

According to Livio (1997) the jet velocity in accreting systems is generally of the order of the escape velocity from the central star. This suggests a lower “i” than for BF Cyg.

HeI line shows evidence of mass loss via wind indicated by strong P-Cyg profiles.

Tomov et al. 2000, A&A, 354, L25

Transient Jets in the Symbiotic Prototype Z Andromedae

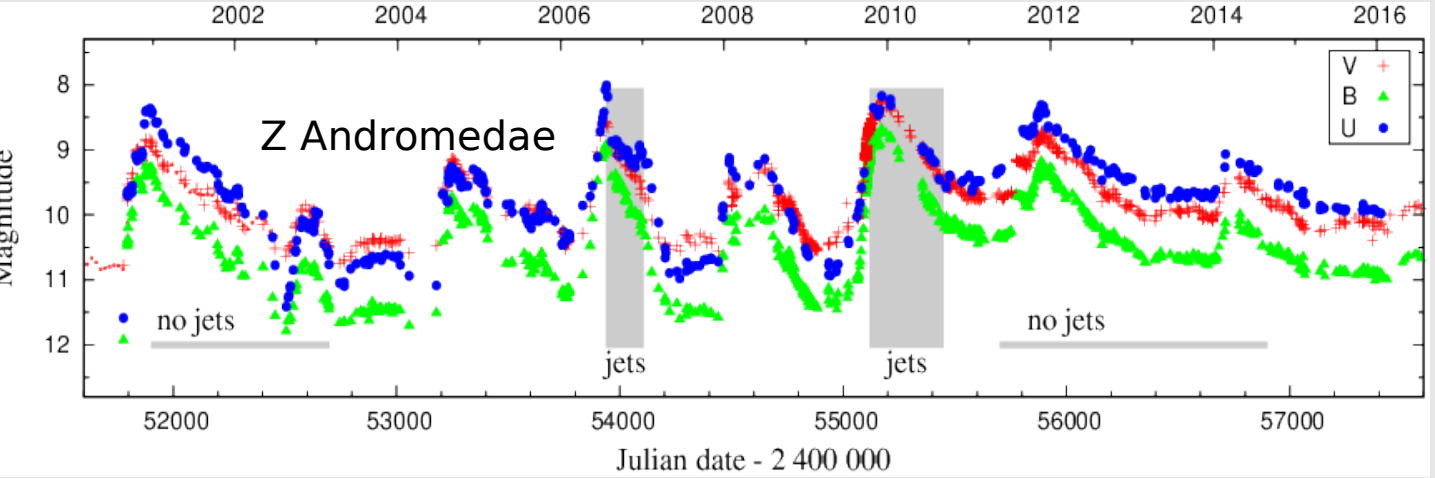

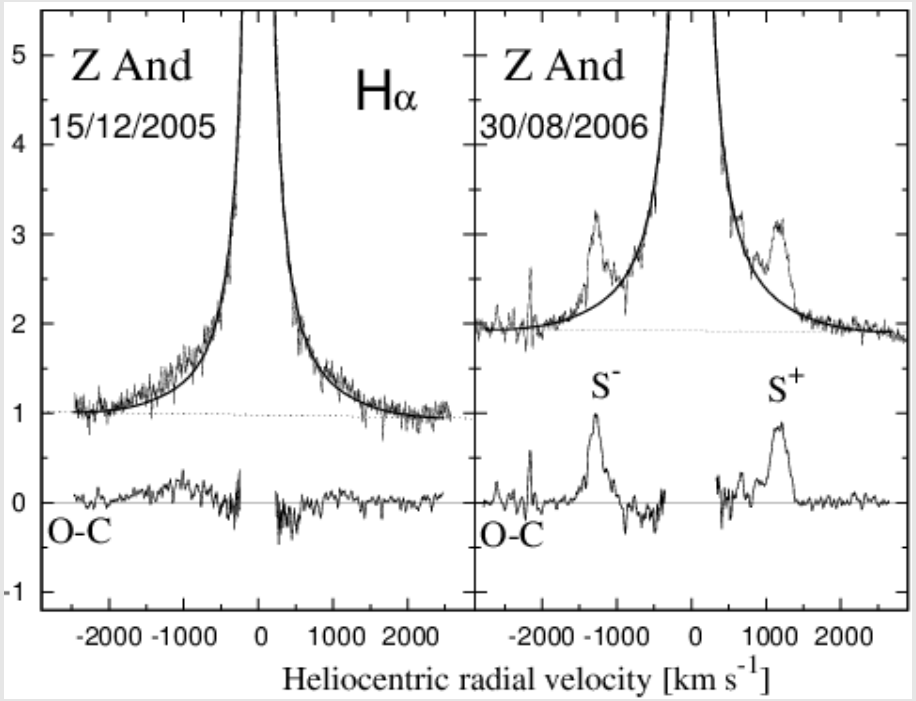

Observed and synthetic Hα profiles from the ion. wind.
dM/dt = 1.3 and 2.5 × 10^{-6} Mo/yr.

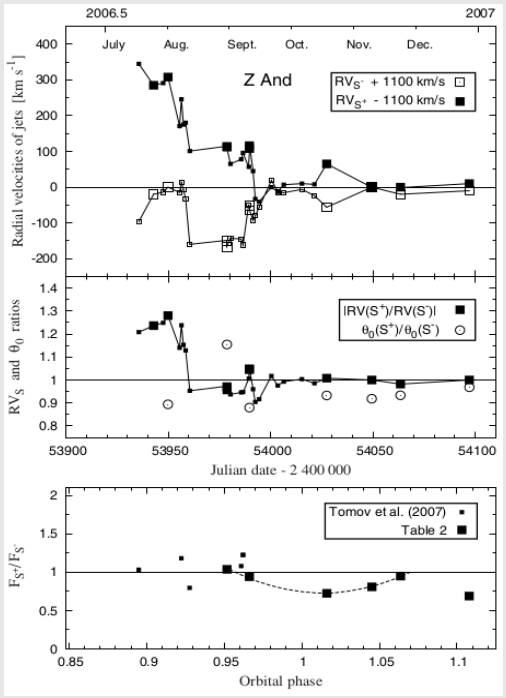

RV_S, θ_0, F_{S+}/F_{S-}
Asymmetry of jets

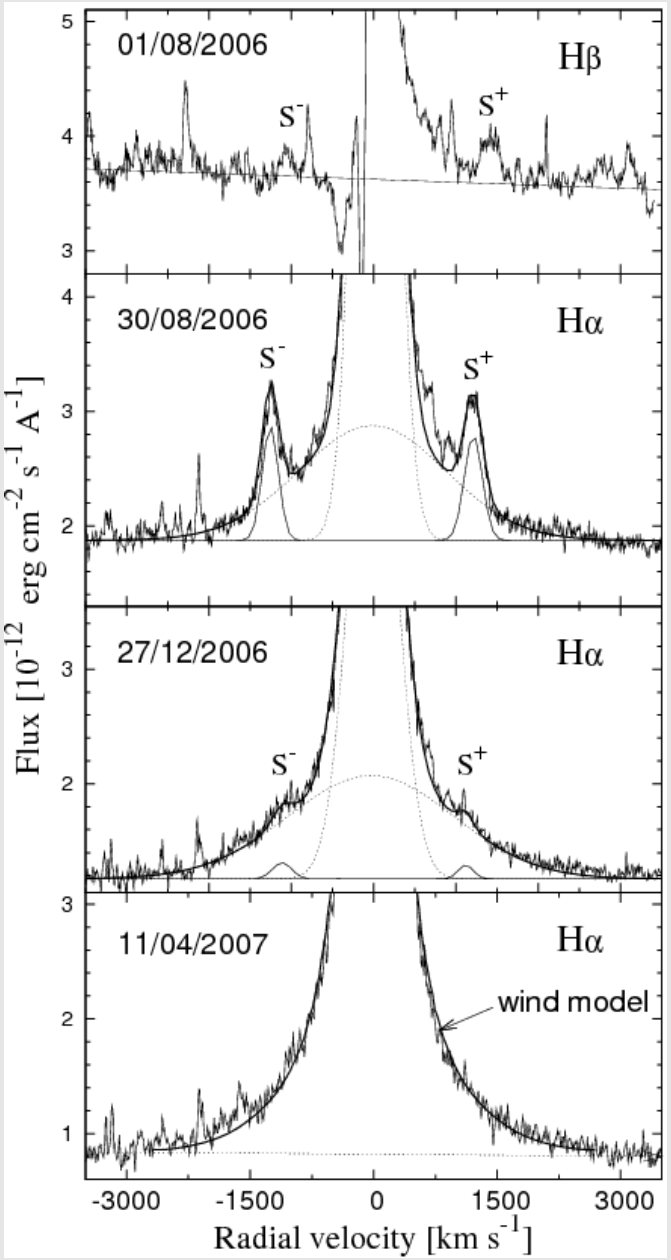

Detection of jets in the spectrum

Skopal, A. et al. 2009, ApJ, 690, 1222

Transient jets from warped disk in Z Andromedae

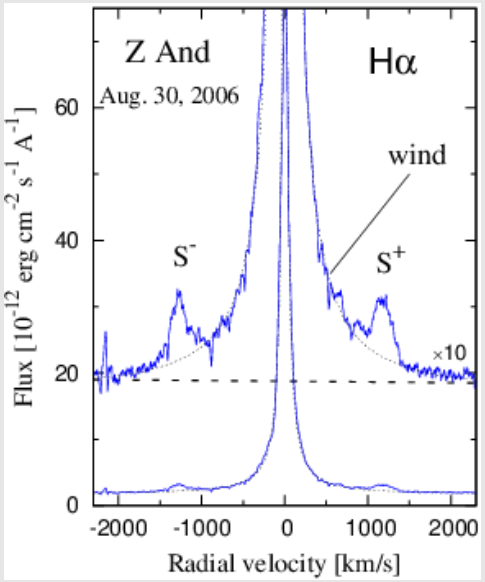

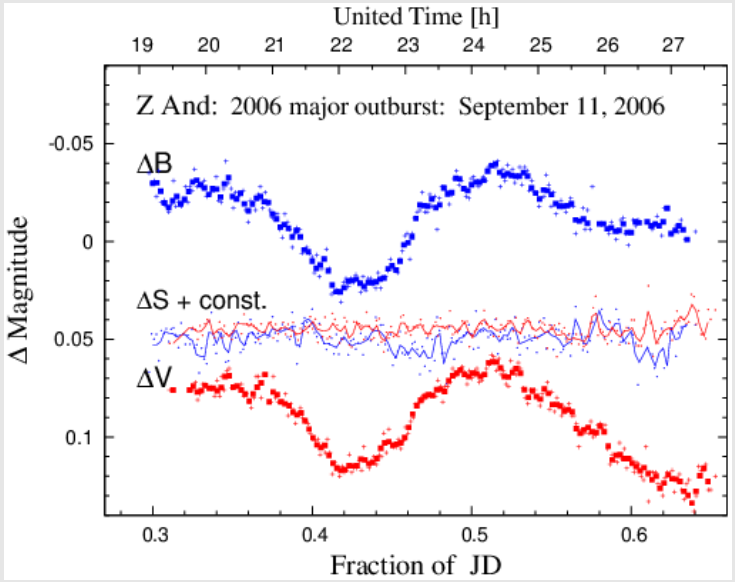

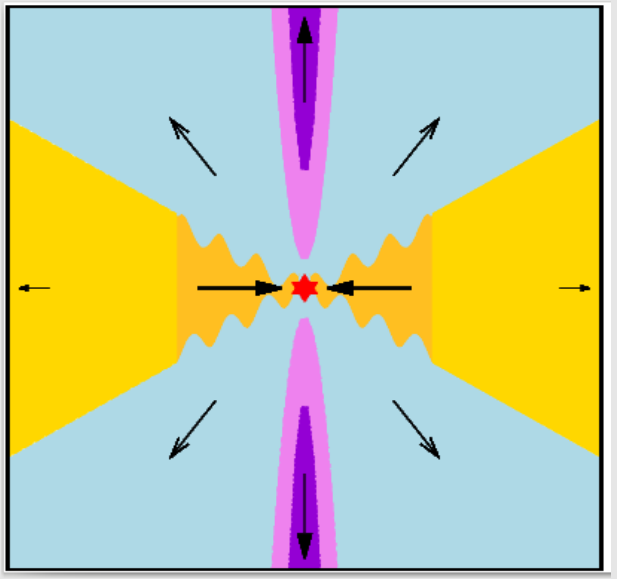

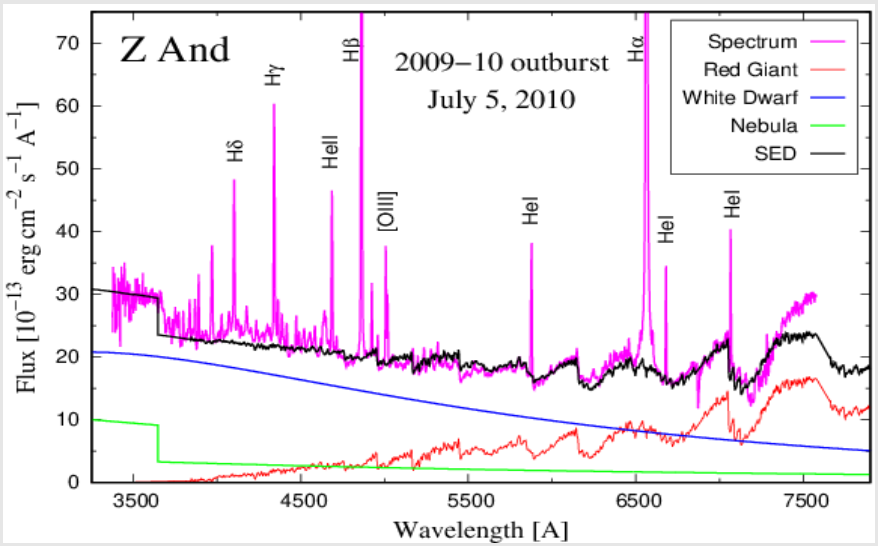

White Dwarf:

$T_{BB} \sim 9000\,\mathrm{K}$, $R_{WD}^{eff} \sim 11\,\mathrm{Ro}$

$\Rightarrow L_{ph}(WD) \sim 3\times10^{42}\,\mathrm{s}^{-1}$

Nebula:

$T_e \sim 30000\,\mathrm{K}$, $EM = 1.7\times10^{60}\,\mathrm{cm}^{-3}$

$$L_{ph}(WD) \ll \alpha_B(H, T_e)\times EM \ \ \mathrm{s}^{-1}$$

WD has a disk-like structure

The **bipolar jets** are indicated by S- and S+ satellite components. Simultaneously, the rapid photometric variation (Δm ~ 0.06 mag) develops. The SED indicates the presence of a large disk-like structure around the WD. **Outburst** → disruption of the inner parts of the disk, which causes wobbling of its outer parts.

Ionization structure during quiescent and active phases of symbiotic stars

SED models

(i) non-eclipsing systems – hot stellar source → hot type outbursts

AG Pegasi

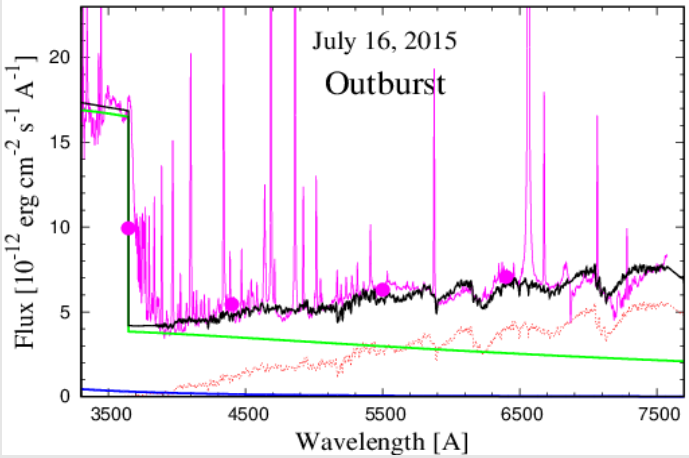

V426 Sagittae

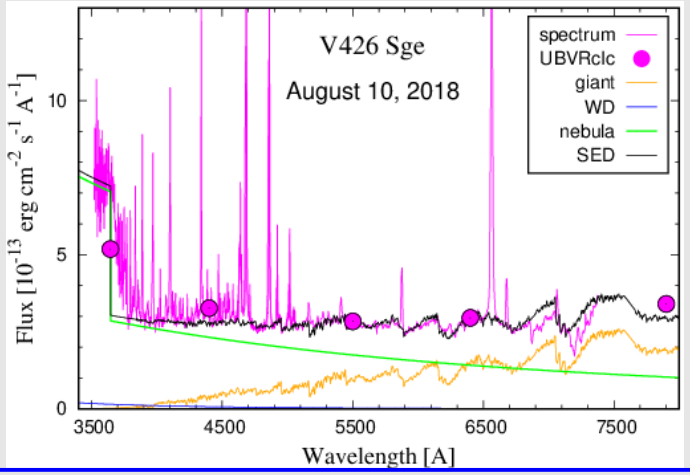

AG Draconis

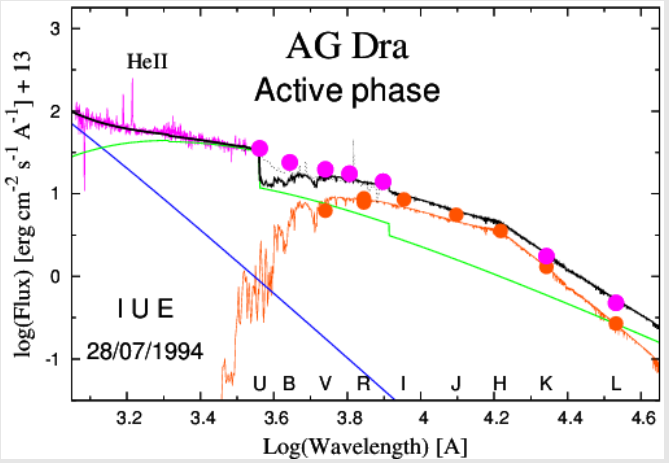

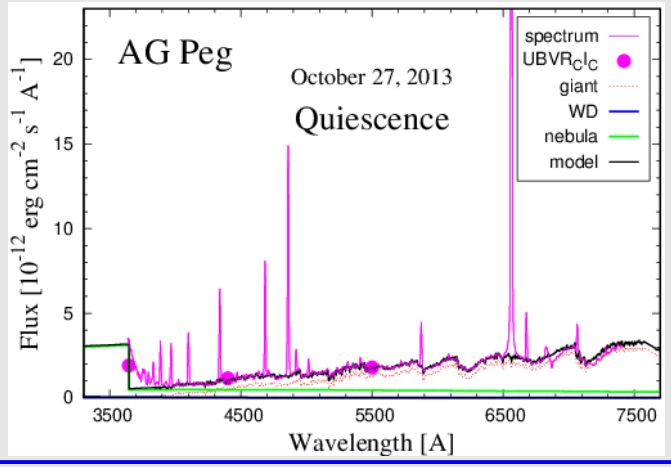

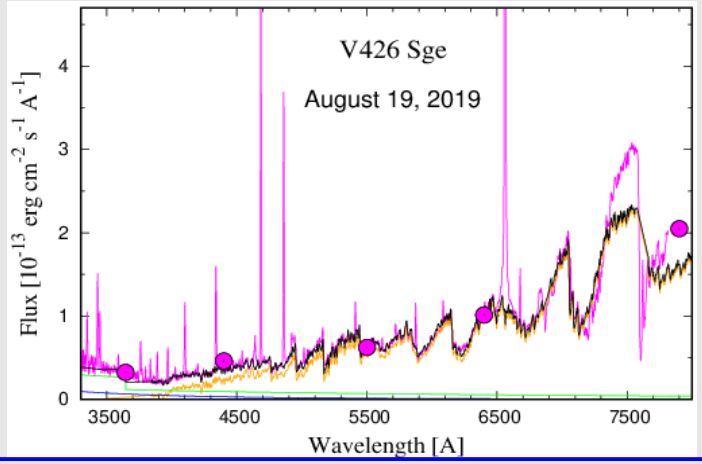

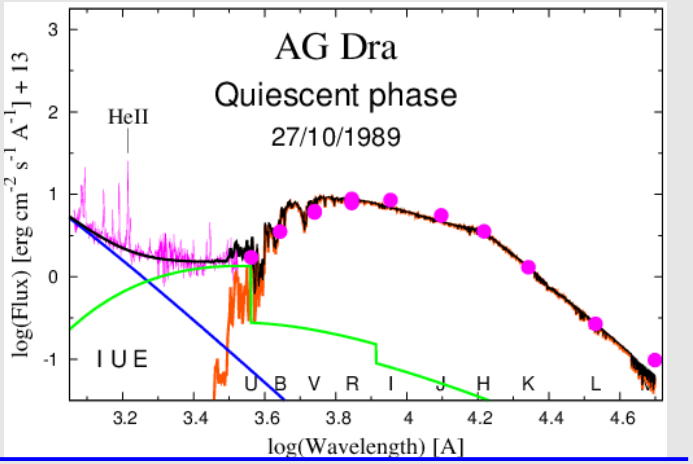

Active phase:

$EM \sim 10^{60-61}\, cm^{-3}$,
$T_{WD} \sim 2\times10^{5}\, K$,
$R_{WD}^{eff} \sim 0.12\, R_{Sun}$,
$L_{WD} \sim$ a few $\times 10^{37}\, erg/s$,
$\dot{M} =$ a few $\times 10^{-6}\, M_{Sun}/\, year$.

Quiescent phase:

$EM \sim a\, few \times 10^{59} cm^{-3}$,
$T_{WD} \sim 1.5\times10^{5}\, K$,
$R_{WD}^{eff} \sim 0.05\, R_{Sun}$,
$L_{WD} \sim$ a few $\times 10^{36}\, erg/s$,
$\dot{M} =$ a few $\times 10^{-8}\, M_{Sun}/\, year$.

SED models

(ii) eclipsing systems – warm stellar source → warm type outbursts

Active phase

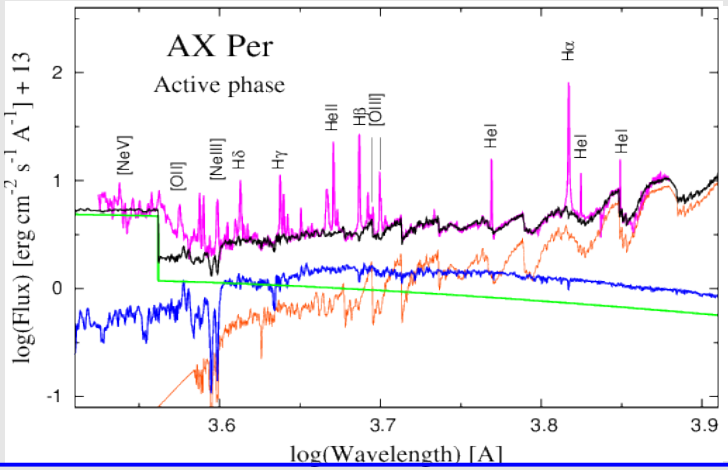

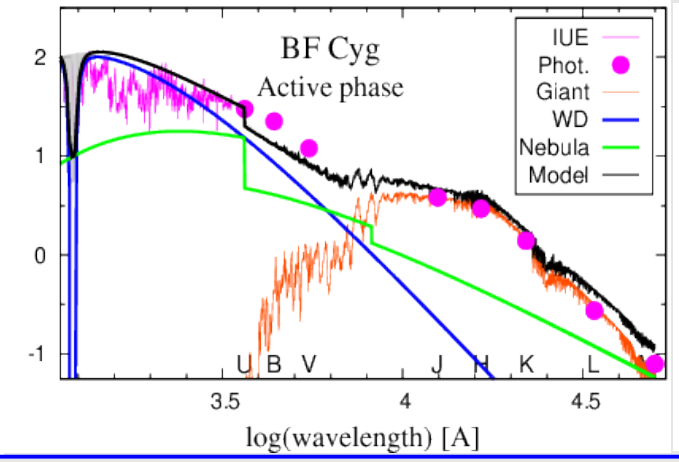

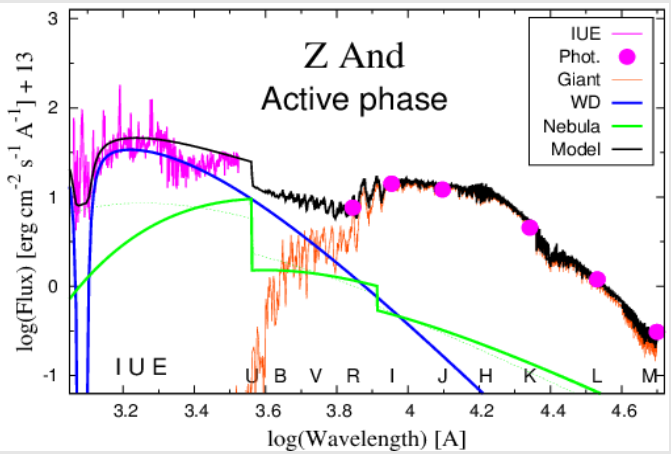

Quiescent phase

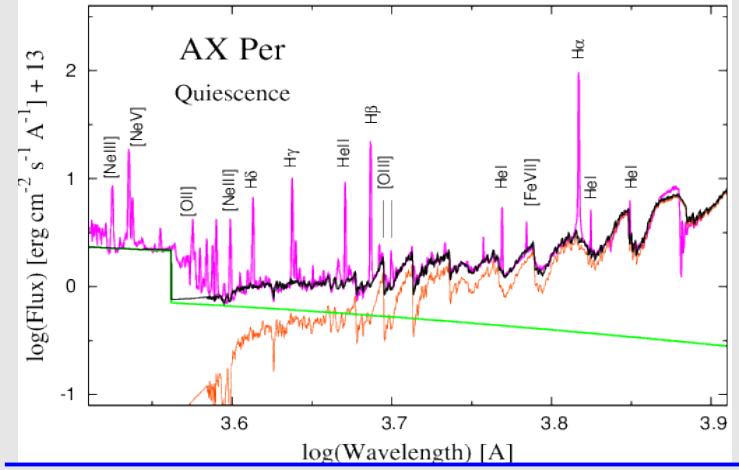

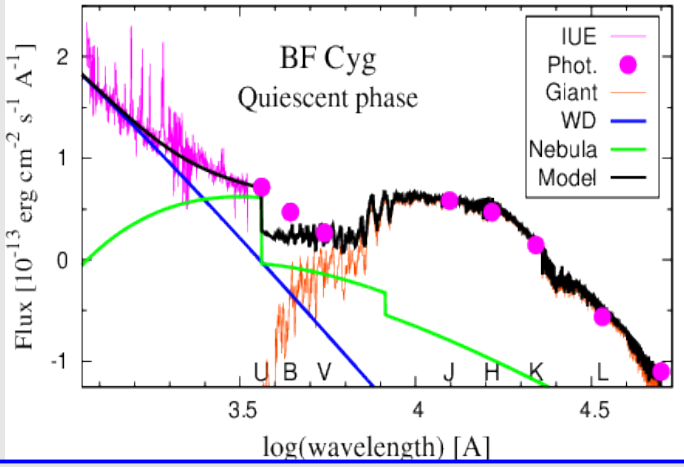

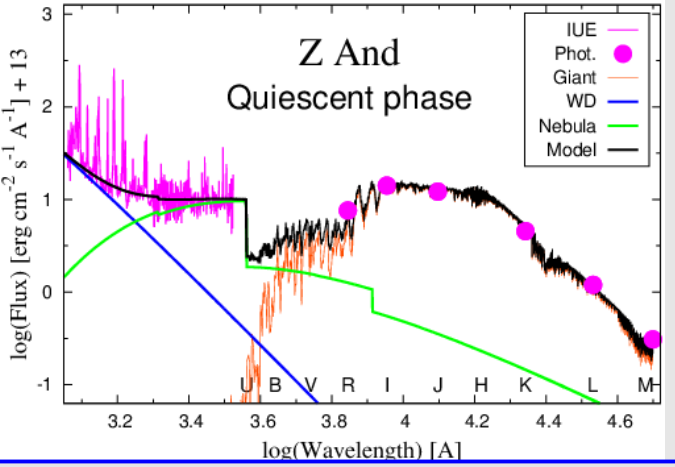

Active phase: Emergence of a warm, 1–3 x 10^4 K, WD's pseudophotosphere with the effective radius of a few x (0.1–1.0) R_{solar} .

But EM ~ 10^{59} – 10^{60} cm^{-3} and emission lines !

Dramatic changes during transition from Quiescent to Active phase:

	Q-phase	→	A-phase
Light curve:	wave-like var.	→	narrow minima (eclipses)
UV-SED: T(WD)	1–2 x 10^5 K	→	1–2 x 10^4 K
EM	~10^{59} cm^{-3}	→	~10^{60} cm^{-3}
Rayleigh scattering	sp. conj.	→	around the orbit

Simultaneous presence of

1. a warm pseudophotosphere (T~1-2 x 10^4 K)
2. a strong nebular emission (EM = $n^p n_e V \sim 10^{60}$ cm^{-3})

The former is not capable of giving rise to the latter component:

$$L_{ph}(\text{shell}) \ll \alpha_B \times EM$$

→ the presence of a hot ionizing source that is not seen by the observer.

The disk-like structure of the hot component

Hot and warm type of outbursts

The disk-like structure around the WD and the neutral region in the orbital plane determine the biconical shaping of the ionized region with the tops at the WD. This is responsible for observing two different types of spectra depending on the orbital inclination:

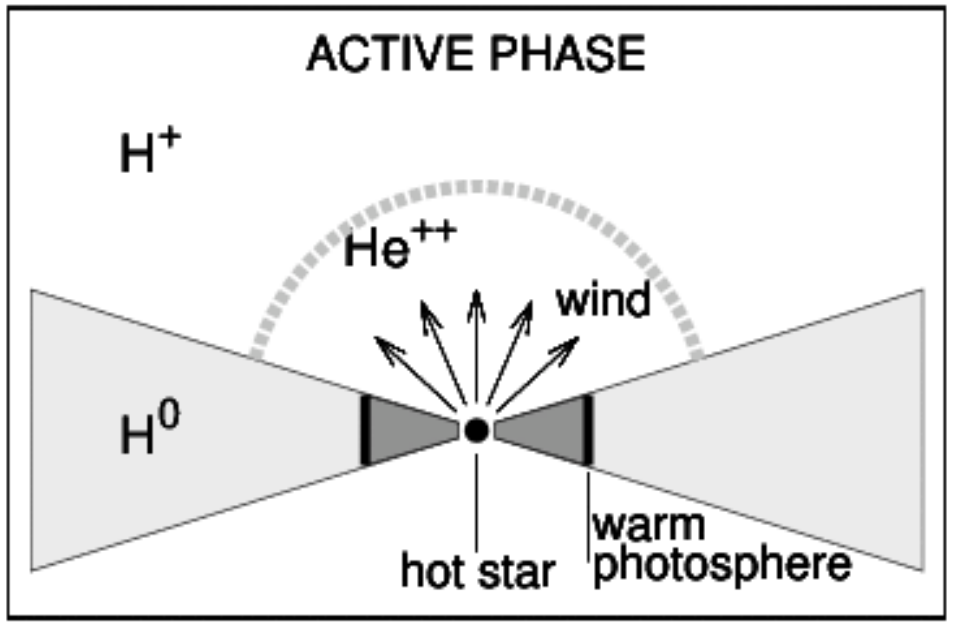

Low "i": hot type outbursts

- the stellar component is hot, negligible in the optical:

  T_{BB} ~ 1.5–2 x 10^5 K, R_h^{eff} ~ 0.1 Ro,

  L_{WD} ~ 5 x 10^{37} erg/s

- nebular component dominates the optical from the very beginning of the outburst (see slide 64). EM ~ 10^{60} cm^{-3},

  Te ~ 30 000 K.

High "i": warm type outbursts

- two-temperature type UV spectrum, strong warm stellar component in the optical (see slides 65, 66),

  T_{BB} ~ 1–3 x 10^4 K.

- two-velocity type of mass outflow from the hot component (slide 70).

Emergence of a neutral region in the orbital plane during Z And type outbursts

The formation of the disk-like structure of the hot component during outbursts of SySts represents the key effect for understanding the symbiotic phenomenon.

Its natural consequence is the simultaneous neutralization of the giant's wind in the orbital plane during outbursts: The flared disk actually blocks ionizing photons from the central hot WD within its vertical extension, which causes the initially ionized wind before the outburst (i.e., during quiescence) to become neutral in the orbital plane during the outburst.

This effect is detectable by Rayleigh scattering on neutral atoms of hydrogen, best observable as a depression of the continuum around the Lyα line. For eclipsing systems, it is measurable at any orbital phase.

fi ~0.5 →

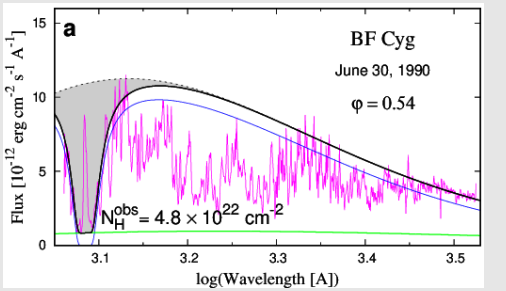

$N_H \sim 5 \times 10^{22}$ cm^{-2}

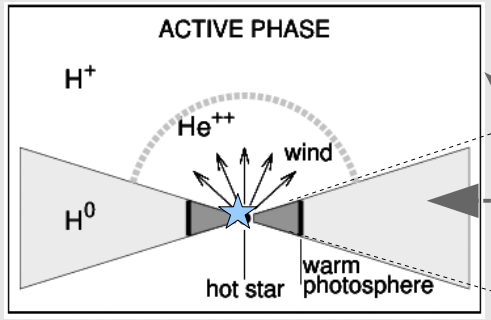

← fi ~0

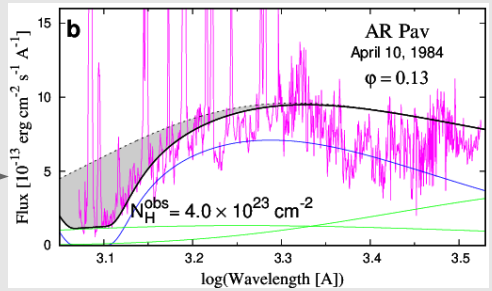

$N_H \sim 1 \times 10^{24}$ cm^{-2}

Neutral wind region in the orbital plane during outbursts of SySts

Eclipsing systems: *Rayleigh scattering during outbursts*: $N_H = 10^{22} - 10^{24}\,\mathrm{cm}^{-2}$. Asymmetry of $N_H(\varphi)$ as in HMXBs.

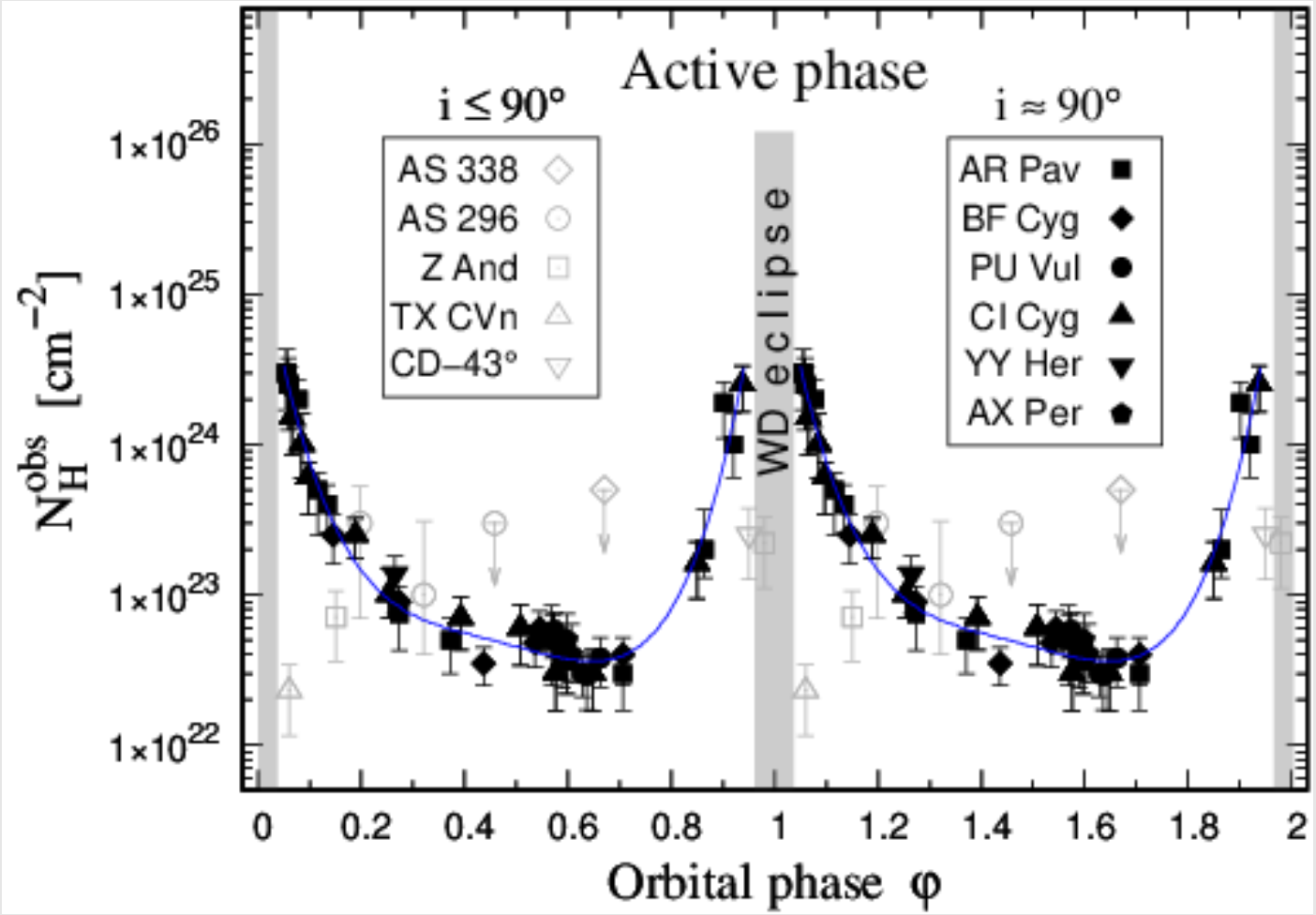

During active phases, a neutral region consisting of wind from the giant emerges in the orbital plane. It is observable here due to the formation of a dense disk-like structure around the WD during outbursts, which blocks ionizing radiation from the central burning WD in the orbital plane. The orbitally-related asymmetry of the measured column densities could be attributed to tidal streams and accretion wakes as for HMXBs.

Skopal, 2023, AJ, 165:258

Challenges for future work

- Acquiring multi-frequency observations covering the widest possible range of the spectrum: more reliable parameters; connections of thermonuclear outbursts in accreting white dwarf binaries.

- Testing theoretical modeling of wind morphology in SySts that meet measured N_H values around their orbits.

- Determine a more accurate mass-transfer mode operating in S-type SySts (i.e., the wind compression model) for the conditions derived from observations ($\dot{M}\left(\theta=\pi/2\right)/\dot{M}\approx 10$, $\dot{M}\approx 10^{-7}\ M_{solar}/yr^{-1}$).

- Implementation of the efficient wind mass-transfer mode in the binary population synthesis codes → a more reliable SySts lifetime and the expected number of SySts in the Milky Way.

- Specific Task: Can the wind material focused on the orbital plane mimic the ellipsoidal light variation observed in the light curves of some SySts?

Thank you for your attention !

Wind-focusing and ellipsoidal light variations

The light curves of many SySts show so-called ellipsoidal variation (e.g., Gromadzki et al. 2013), which is generally understood to be a result of the Roche-lobe filling giant.

However, there are arguments against this natural interpretation. For example:

1. For 30 SySts, Mürset & Schmid (1999) found that $R_{RG} \leq l_1/2$, where $l_1 = r(L_1)$ – RG(center). Only exception is T CrB.

2. The SySt **V1261 Ori** (P_{orb} ~ 638 d, R_{RL} ~ 200 R_{Sun}) shows a pronounced ellipsoidal variation, but the interferometric measurements suggest R_{RG}/R_{RL} ~ 0.3 (Boffin et al. 2014).

3. The largest discrepancy between R_{RG} and R_{RL} is most apparent for some yellow SySts. For example,
   - **LT Del**: P_{orb} = 479 d, a ~ 314 R_{Sun}, R_{RL} ~ 138 R_{Sun}
     G6III, R_{RG} ~ 10 R_{Sun}
   - **IV Vir**: P_{orb} = 282 d, a ~ 220 R_{Sun}, R_{RL} ~ 97 R_{Sun}
     K2III, R_{RG} ~ 20 R_{Sun}

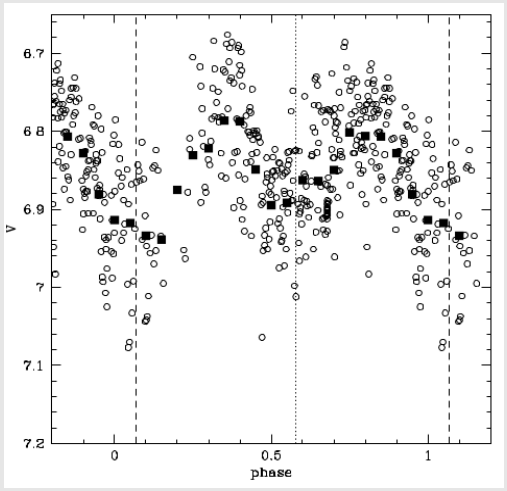

ASAS-V LC of V1261 Ori
(Boffin et al. 2014, A&A, 564, A1)

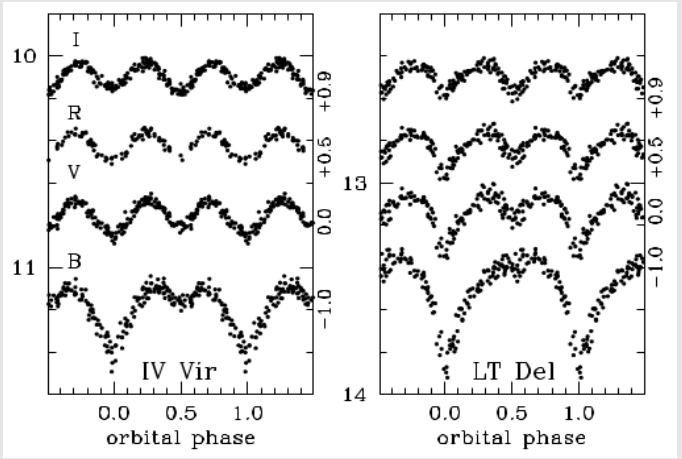

BVRI LCs of IV Vir and LT Del
(Munari, U., 2019, CAS, 54, 77)

→

Roche-lobe overflow in SySts is not unambiguously proved by the ellipsoidal light variations.

Raman scattering

Example of the AG Draconis spectrum
covering the Hα – OVI Raman scattered emission

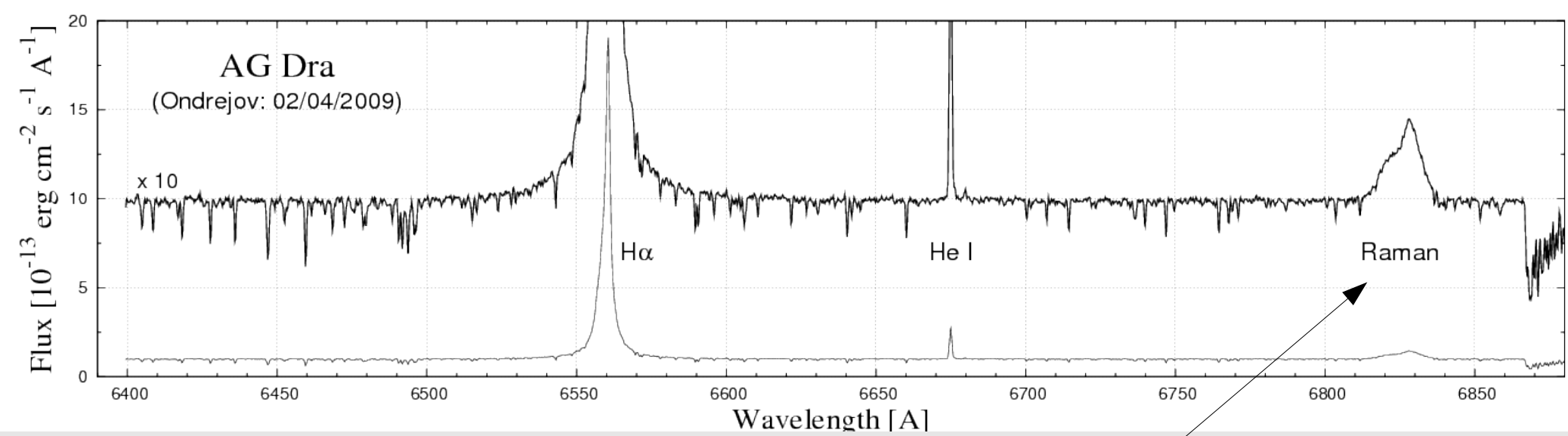

Ly-β ... 1025.728, OVI ... 1031.912

$\Delta\lambda_{OVI} \sim 6.184$ A ... if $\Delta\lambda \sim 0$

$\Delta\lambda_{Ram} = \lambda_{OVI}(Ram) - \lambda_{H\alpha} \sim 270.5$ A

$\lambda_{Ram} \sim 6830$ A